Published by Institute of Physics Publishing for SISSA

Received: *April 11, 2008*
Accepted: *May 30, 2008*
Published: *June 23, 2008*

Lepton flavour violating semileptonic τ decays in constrained MSSM-seesaw scenarios

Ernesto Arganda and Maria J. Herrero

Departamento de Física Teórica and Instituto de Física Teórica, IFT-UAM/CSIC
Universidad Autónoma de Madrid, Cantoblanco, E-28049 Madrid, Spain
E-mail: ernesto.arganda@uam.es, maria.herrero@uam.es

Jorge Portolés

IFIC, Universitat de València - CSIC,
Apt. Correus 22085, E-46071 València, Spain
E-mail: jorge.portoles@ific.uv.es

Abstract: In this work we study the Lepton Flavour Violating semileptonic τ decays: 1) $\tau \to \mu PP$ with $PP = \pi^+\pi^-, \pi^0\pi^0, K^+K^-, K^0\bar{K}^0$; 2) $\tau \to \mu P$ with $P = \pi^0, \eta, \eta'$ and 3) $\tau \to \mu V$ with $V = \rho^0, \phi$. We work within the context of two constrained MSSM scenarios: the CMSSM-seesaw and NUHM-seesaw, with a MSSM spectrum extended by three ν_R and their SUSY partners and where the seesaw mechanism for neutrino mass generation is implemented. A full SUSY one-loop computation is presented and the importance of the various contributions, the γ-, Z-, and Higgs bosons mediated ones, are analysed. The hadronisation of quark bilinears is performed within the chiral framework. Some discrepancies in the predicted rates for BR($\tau \to \mu\eta$), BR($\tau \to \mu\eta'$) and BR($\tau \to \mu K^+K^-$) are found with respect to previous estimates, which will be commented here. These three channels will be shown to be the most competitive ones to test simultaneously the Lepton Flavour Violation and the Higgs sector. We further present here a set of approximate formulas for all the semileptonic channels which we believe can be useful for further comparison with present and future data.

Keywords: Higgs Physics, Rare Decays, Neutrino Physics, Supersymmetric Standard Model.

JHEP06(2008)079

Contents

JHEP06(2008)079

1. Introduction

Lepton Flavour Violating (LFV) processes provide one of the most challenging tests of supersymmetric (SUSY) extensions of the Standard Model (SM) of Particle Physics [1–4]. One of the most popular ones among these extensions is the Minimal Supersymmetric Standard Model (MSSM) enlarged with three right handed neutrinos and their corresponding SUSY partners, and where the physical neutrino masses are generated via a seesaw mechanism [5, 6]. Within this SUSY-seesaw context, the light neutrino masses and neutrino mixing angles can be easily accommodated in agreement with present data [7] by setting appropriate input values for the heavy right handed neutrino masses, within the range $M_R \sim (10^{10} - 10^{15})\,\text{GeV}$, and appropriate Yukawa couplings, Y_ν. The hypothesis of Majorana neutrinos is crucial in this concern, because it is only for them that large Yukawa couplings, say $Y_\nu \sim \mathcal{O}(1)$, can be set. An interesting connection between neutrino and LFV physics then follows, because the large Yukawa couplings induce, via loops of SUSY

particles [8], important contributions to the rare LFV processes. In fact, these contributions are in some cases, already at the reach of their present experimental sensitivity. So far, the most sensitive LFV process to the Yukawa couplings in the SUSY-seesaw context is $\mu \to e\gamma$, where the present experimental sensitivity is at 1.2×10^{-11} [9, 10]. In the future, if the announced improvement in the sensitivity of $\mu - e$ conversion in nuclei of up to 10^{-18} is finally reached [11], this process will be by far the most competitive one. Regarding the tests of Lepton Flavour Violation (LFV) in the $\tau - \mu$ sector, the most competitive one at present is $\tau \to \mu\gamma$, whose upper bound is now set to 1.6×10^{-8} [12 – 15]. Furthermore, the sensitivity to LFV in $\tau \to 3\mu$ has also improved notably in the last years. The present upper bounds from BELLE and BABAR collaborations are 3.2×10^{-8} [16] and 5.3×10^{-8} [17], respectively. This leptonic channel has the advantage over the radiative $\tau \to \mu\,\gamma$ decay that provides a test not only of SUSY but also of the Higgs sector. It is remarkable that both $\tau \to 3\mu$ decay [18 – 22] and $\mu - e$ conversion [23, 24] in nuclei can get important contributions from Higgs mediated diagrams in SUSY scenarios with large $\tan\beta$ and light MSSM Higgs bosons.

In the present work, we study the LFV semileptonic tau decay channels which are also of interest because of the recently reported sensitivity by BELLE and BABAR collaborations [25 – 28] that are, for some channels, already competitive with the LFV tau leptonic ones. In particular we analyse here the following semileptonic tau decays: 1) $\tau \to \mu PP$ with $PP = \pi^+\pi^-, \pi^0\pi^0, K^+K^-, K^0\bar{K}^0$; 2) $\tau \to \mu P$ with $P = \pi^0, \eta, \eta'$ and 3) $\tau \to \mu V$ with $V = \rho^0, \phi$. Their present upper experimental bounds (90% CL) are summarised in table 1. We perform a full one-loop computation of the rates for all these processes within the context of two constrained SUSY-seesaw scenarios which are of particular interest: The usual constrained MSSM-seesaw (CMSSM-seesaw) scenario [29], with universal soft SUSY masses at the gauge coupling unification scale, and the so-called Non-Universal Higgs Mass (NUHM) scenario [30], with all those soft masses being universal except for the Higgs sector ones. In this later case the predicted Higgs particle masses can be low, indeed close to their present experimental lower bounds (for the SM Higgs the present bound is $m_H > 114.4\,\text{GeV}$ 95% C.L. [7]), and the corresponding Higgs-mediated contribution to the previous LFV processes can be relevant, even for large soft SUSY masses.

In the previous related literature there are, to our knowledge, just a few theoretical computations of some of these LFV semileptonic τ decays induced by SUSY loops. In particular, $\tau \to \mu\eta$ was first computed in [31] within the context of the unconstrained MSSM and in the approximation of large $\tan\beta$. A more refined analysis of this channel, $\tau \to \mu\eta'$, $\tau \to \mu\pi$, and $\tau \to \mu\rho$ was done in [32] for the unconstrained MSSM scenario and large $\tan\beta$ approximation as well, but they used an effective lagrangian framework for the LFV operators. An estimate of $\tau \to \mu\eta$ with the use of the mass insertion (MI) approximation for the relevant lepton flavour mixing parameter between the τ and μ sectors, δ_{32}, has been performed in [33]. The decay mode $\tau \to \mu K^+K^-$ has been estimated in [34] within the mass insertion and leading logarithmic (LLog) approximations for δ_{32}, and taking into account only the Higgs-mediated contribution in the large $\tan\beta$ limit. In all these previous works no connection with the neutrino sector was considered and the hadronisation of quark bilinears in the final state is simply parameterised in terms of the proper meson

JHEP06(2008)079

decay constants and meson masses. Other estimates of some of these LFV semileptonic τ decays in different contexts, like SO(10)-SUSY-GUT model with universal soft breaking terms [35] and Littlest Higgs model [36], have also been performed in the literature.

Our analysis presented here is more complete in several aspects. First, we include both Z-boson and A^0-boson mediated contributions to $\tau \to \mu P$ ($P = \eta, \eta', \pi^0$), and both γ and H^0, h^0-bosons mediated contributions to $\tau \to \mu K^+ K^-$. The other channels, $\tau \to \mu K^0 \bar{K}^0$ and $\tau \to \mu \pi^0 \pi^0$ have not been estimated previously. We include γ and H^0, h^0-bosons mediated contributions in $\tau \to \mu K^0 \bar{K}^0$. The case $\tau \to \mu \pi^0 \pi^0$ can only be mediated by H^0, h^0-bosons. Second, we do not use either the mass insertion nor the LLog approximation and our analytical computation is valid for all $\tan\beta$ values. Third, we make a connection with neutrino physics by requiring compatibility through all this work with the neutrino data for masses and mixing angles. Fourth, we perform the hadronisation of quark bilinears with close attention to the chiral constraints, guided by the resonance chiral theory [37] that has proven to be a robust framework for the analyses of hadrodynamics when resonances are involved. The γ amplitude, due to its pole at $q^2 = 0$, is most sensitive to the hadronisation procedure. Hence the hadronisation of the electromagnetic current, that drives the γ contributions, has been carried out by a careful construction of the vector form factor that matches both the chiral low-energy limit and the asymptotic smoothing at high q^2 [38]. Those final states driven by heavy intermediate bosons like the Z^0 or Higgses, on the other side, do not require such an involved scheme. In these cases we have used the leading chiral approximation of Chiral Perturbation Theory that we know, for sure, it has to be fulfilled by the hadronisation. The advantage of our approach is that it provides the most successful description up to date of the hadronic tau decays and it can be systematically improved by further developments of the appropriate form factors, whether axial-vector, scalar or pseudoscalar cases.

The rest of this paper is organised as follows. The theoretical framework for the computation of LFV semileptonic τ decays is described in section 2. This includes a short review of the SUSY-seesaw scenarios that we work within, CMSSM and NUHM, and a description of our procedure for hadronisation of quark bilinears within the context of Chiral Perturbation Theory (χPT) and Resonance Chiral Theory (RχT). In section 3, the analytical results of the full one-loop branching ratios BR($\tau \to \mu PP$), BR($\tau \to \mu P$), BR($\tau \to \mu \rho$) and BR($\tau \to \mu \phi$) are presented. Section 4 is devoted to the numerical results and discussion. It includes, in addition a comparison between the full one-loop and approximate results. A set of useful approximate formulas for the semileptonic tau decay rates that are valid at large $\tan\beta$ are derived. A critical comparison with previous predictions in the literature is also included in this section 4. Finally, section 5 summarises the conclusions.

2. Framework for LFV semileptonic τ decays

In this section we describe the theoretical framework for the computation of the LFV semileptonic τ decay rates. First we present the scenario for the generation of LFV in the

JHEP06(2008)079

LFV semilep. τ decays	BABAR	Belle	BABAR & Belle
BR($\tau \to \mu\eta$)	1.5×10^{-7} [27]	6.5×10^{-8} [26]	5.1×10^{-8} [15]
BR($\tau \to \mu\eta'$)	1.4×10^{-7} [27]	1.3×10^{-7} [26]	5.3×10^{-8} [15]
BR($\tau \to \mu\pi$)	1.1×10^{-7} [27]	1.2×10^{-7} [26]	5.8×10^{-8} [15]
BR($\tau \to \mu\rho$)	—	2.0×10^{-7} [25]	—
BR($\tau \to \mu\phi$)	—	1.3×10^{-7} [39]	—
BR($\tau \to \mu\pi^+\pi^-$)	—	4.8×10^{-7} [25]	—
BR($\tau \to \mu\pi^0\pi^0$)	—	—	—
BR($\tau \to \mu K^+ K^-$)	—	8.0×10^{-7} [25]	—
BR($\tau \to \mu K^0 \bar{K}^0$)	—	—	—

Table 1: Present upper bounds for LFV semileptonic τ decays.

τ-μ sector, then we summarise the main ingredients to perform the hadronisation of quark bilinears within the context of χPT and RχT.

2.1 LFV in the SUSY-seesaw scenario

The SUSY-seesaw scenario that we work within contains the full MSSM spectra and, in addition, the three right handed neutrinos and their SUSY partners. It is defined in terms of both the SUSY and neutrino sector parameters which are summarised in the following.

Regarding the SUSY sector we choose to work in two different constrained MSSM scenarios: The usual Constrained MSSM (CMSSM) with similar input parameters as in mSUGRA models, and the so-called Non-Universal Higgs Mass (NUHM) scenarios with two additional parameters defining the non-universal soft Higgs masses. The corresponding sets of input parameters in these two scenarios are:

$$\begin{aligned} \text{CMSSM} &: M_0\,, M_{1/2}\,, A_0\,, \tan\beta\,, \text{sign}(\mu)\,, \\ \text{NUHM} &: M_0\,, M_{1/2}\,, A_0\,, \tan\beta\,, \text{sign}(\mu)\,, M_{H_1}, M_{H_2}, \end{aligned} \tag{2.1}$$

where M_0, $M_{1/2}$ and A_0 are the universal soft SUSY breaking scalar masses, gaugino masses and trilinear couplings at the gauge coupling unification scale, $M_X = 2 \times 10^{16}$ GeV. Notice that M_0 and A_0 define also the soft parameters in the sneutrino sector. The other CMSSM parameters are, as usual, the ratio of the two Higgs vacuum expectation values, $\tan\beta = v_2/v_1$, and the sign of the μ parameter, sign(μ). The departure from universality in the soft Higgs masses of the NUHM is parameterised in terms of two parameters δ_1 and δ_2 by,

$$M_{H_1}^2 \,=\, M_0^2\,(1+\delta_1)\,, \quad M_{H_2}^2 \,=\, M_0^2\,(1+\delta_2)\,. \tag{2.2}$$

Notice that with the choice $\delta_{1,2} = 0$ one recovers the universal case defined by the CMSSM scenario. For simplicity, and to further reduce the number of input parameters, in all the numerical estimates of this work we will take $M_0 = M_{1/2} \equiv M_{\rm SUSY}$, $A_0 = 0$ and sign(μ) = +1.

JHEP06(2008)079

To evaluate these two sets of parameters at low energies (taken here as the Z gauge boson mass m_Z) we solve the full one-loop Renormalisation Group Equations (RGEs) including the extended neutrino and sneutrino sectors. For this and the computation of the full spectra at the low energy we use here the public FORTRAN code SPheno [40].

Regarding the neutrino sector, we use the seesaw mechanism for neutrino mass generation which is implemented here to the case of three right handed neutrinos. The usual input parameters in this case are the three right handed Majorana masses, $M_{R_{1,2,3}}$ and the neutrino Yukawa coupling 3x3 matrix, Y_ν. The Dirac neutrino mass matrix is then related to the Yukawa couplings by $m_D = Y_\nu\, v_2$, where $v_2 = v \sin\beta$ and $v = 174\,\mathrm{GeV}$. In this seesaw scenario, the physical Majorana neutrinos consist of three light ones, $\nu_{1,2,3}$, with predicted masses being typically $m_{\nu_{1,2,3}} \sim \mathcal{O}(m_D^2/M_R)$, and three heavy ones, $N_{1,2,3}$, with masses $m_{N_{1,2,3}} \simeq M_{R_{1,2,3}}$. However, instead of this we will use another set of input parameters which are more convenient to accommodate the experimental data on light neutrino masses and generational mixing angles. Within this parameterisation, the Dirac mass matrix and, hence, the Yukawa coupling matrix, are derived in terms of the physical neutrino masses, neutrino mixings and a generic complex orthogal 3×3 matrix, R, as follows [41],

$$m_D = Y_\nu\, v_2 = i\sqrt{m_N^{\rm diag}}\, R\, \sqrt{m_\nu^{\rm diag}}\, U_{\rm MNS}^\dagger\,, \tag{2.3}$$

where,

$$m_N^{\rm diag} = {\rm diag}\,(m_{N_1}, m_{N_2}, m_{N_3})\,, \tag{2.4}$$

$$m_\nu^{\rm diag} = {\rm diag}\,(m_{\nu_1}, m_{\nu_2}, m_{\nu_3})\,, \tag{2.5}$$

and we use the standard parameterisation for the unitary matrix $U_{\rm MNS}$ [42, 43] containing the three generational mixing angles θ_{12}, θ_{13} and θ_{23} and the three CP violating phases, δ, $\phi_{1,2}$. In turn, the R matrix is parameterised in terms of three complex angles, θ_i $(i = 1, 2, 3)$ as [41]

$$R = \begin{pmatrix} c_2\, c_3 & -c_1\, s_3 - s_1\, s_2\, c_3 & s_1\, s_3 - c_1\, s_2\, c_3 \\ c_2\, s_3 & c_1\, c_3 - s_1\, s_2\, s_3 & -s_1\, c_3 - c_1\, s_2\, s_3 \\ s_2 & s_1\, c_2 & c_1\, c_2 \end{pmatrix}\,, \tag{2.6}$$

with $c_i \equiv \cos\theta_i$ and $s_i \equiv \sin\theta_i$. One interesting aspect of this matrix is that it encodes the possible extra neutrino mixings (associated with the right-handed sector) in addition to the ones in $U_{\rm MNS}$. Notice also that the previous eq. (2.3) is established at the right-handed neutrino mass scale M_R, so that the quantities appearing in it are indeed the renormalised ones, namely, $m_\nu^{\rm diag}(M_R)$ and $U_{\rm MNS}(M_R)$. These latter are obtained here by means of the RGEs and by starting the running from their corresponding renormalised values at m_Z, $m_\nu^{\rm diag}(m_Z)$ and $U_{\rm MNS}(m_Z)$ which are identified respectively with the physical $m_\nu^{\rm diag}$ and $U_{\rm MNS}$ from neutrino data.

Concerning our choice for the size of the physical neutrino parameters, we shall focus in this work on scenarios where both light and heavy neutrinos are hierarchical,

$$m_{\nu_1} \ll m_{\nu_2} \ll m_{\nu_3}\,,$$
$$m_{N_1} \ll m_{N_2} \ll m_{N_3}\,,$$

and set the numerical values for the light neutrino parameters to the following ones which are compatible with present data [7, 44]

$$m^2_{\nu_1} \simeq 0\,, \qquad m^2_{\nu_2} = \Delta m^2_{\rm sol} = 8 \times 10^{-5}\ {\rm eV}^2\,, \qquad m^2_{\nu_3} = \Delta m^2_{\rm atm} = 2.5 \times 10^{-3}\ {\rm eV}^2\,,$$
$$\theta_{12} = 30^\circ\,, \qquad \theta_{23} = 45^\circ\,, \qquad \theta_{13} \simeq 0, \qquad \delta = \phi_1 = \phi_2 = 0\,. \tag{2.7}$$

Notice that, for simplicity, the three CP violating phases, have been set to zero. We have also set to zero the θ_{13} mixing angle and the lightest neutrino mass in order to minimise as much as possible the LFV in the $\mu - e$ sector. In fact, we have checked that for the explored parameters region in this work, this $\mu - e$ LFV is below the sensitivity of the present data from $\mu \to e\gamma$, $\mu \to 3e$ and $\mu - e$ conversion in nuclei.

In summary, the input parameters of the neutrino sector for the present work are:

$$\text{Seesaw}: m_{N_{1,2,3}}\ \ ,\ \ \theta_{1,2,3}\,. \tag{2.8}$$

Regarding the generation of LFV in these constrained MSSM scenarios, we remind that all lepton flavour mixing originates solely from the neutrino Yukawa couplings. These Y_ν first induce flavour violation in the slepton sector by the RGE running of the soft SUSY breaking parameters from M_X down to the electroweak scale m_Z. It is manifested in the non-vanishing values of the off-diagonal elements of the slepton squared mass matrix at m_Z. We perform this running by solving the full set of one-loop RGEs including the neutrino and sneutrino sectors. The resulting slepton mass matrices at m_Z are then diagonalised and the previous flavour mixing is then transmitted to the mass eigen-values and eigen-states. Therefore, in this work where we deal with physical states, all flavour mixing is implicit in the resulting physical charged slepton masses, $m^2_{\tilde{l}_1}, \ldots, m^2_{\tilde{l}_6}$, sneutrino masses, $m^2_{\tilde{\nu}_1}$, $m^2_{\tilde{\nu}_2}$, $m^2_{\tilde{\nu}_3}$ and the corresponding matrices that rotate from the electroweak to the slepton and sneutrino mass bases, respectively, R^l and R^ν. The LFV in the physical processes, like $l_j \to l_i\gamma$, $l_j \to 3l_i$, $\mu - e$ conversion in nuclei, and the semileptonic τ decays studied here, are then generated by the SUSY one-loop contributing diagrams that contain these slepton physical masses in the internal propagators, and also the previous rotation matrices in the interaction vertices, which connect between different lepton generations. A complete set of Feynman rules for the relevant LFV vertices can be found in [21, 24].

Finally, in order to illustrate more quantitatively how important can be the size of the flavour mixing between the stau and smuon sectors, in the CMSSM-seesaw scenario, we include next the predictions of the mixing parameter δ_{32} that is defined in the LLog approximation as,

$$\delta_{32} = -\frac{1}{8\pi^2}\frac{(3\,M_0^2 + A_0^2)}{M^2_{\rm SUSY}}\left(Y_\nu^\dagger\, L\, Y_\nu\right)_{32}\,, \tag{2.9}$$

where L is a 3×3 diagonal matrix whose elements are, $L_{ii} = \log(M_X/m_{N_i})$ and $M_{\rm SUSY}$ is an average SUSY mass. This phenomenological parameter δ_{32} measures the amount of flavour mixing between the second and third slepton generations in the left-handed sector (LL), which is by far the dominant one. The corresponding mixing in the right-handed slepton sector is extremely suppressed by the smallness of the lepton masses which appear as global factors in the definitions of those (RR and RL) mixings (see, for instance, [21]).

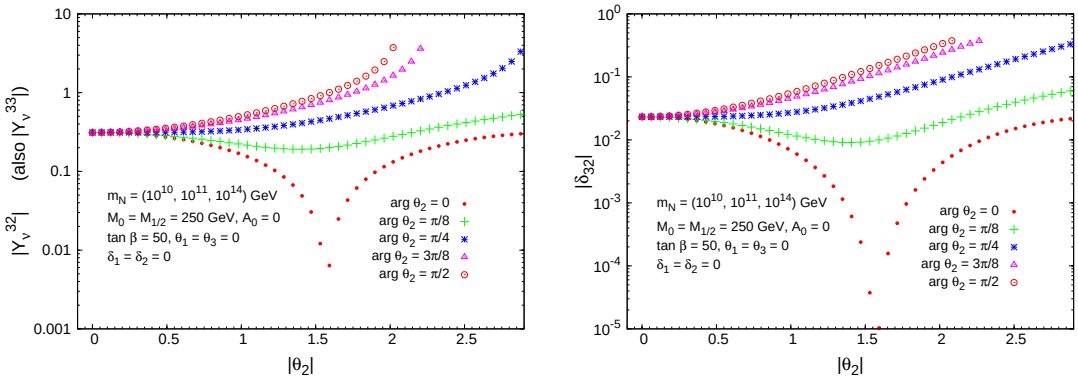

Figure 1: $|Y_\nu^{32}|$ and $|\delta_{32}|$, in the CMSSM-seesaw scenario, as a function of $|\theta_2|$, for $\arg\theta_2 = \{0, \pi/8, \pi/4, 3\pi/8, \pi/2\}$ (dots, crosses, asterisks, triangles and circles, respectively). Both $|\theta_2|$ and $\arg\theta_2$ are given in radians. The predictions for $|Y_\nu^{33}|$ are practically indistinguishable from those for $|Y_\nu^{32}|$.

One can estimate δ_{32} from the previous parameterisation of the seesaw model in eq. (2.3) by simply plugging in eq. (2.9) the value of $\left(Y_\nu^\dagger\, L\, Y_\nu\right)_{32}$ from the following expression,

$$
\begin{aligned}
v_2^2 \left(Y_\nu^\dagger\, L\, Y_\nu\right)_{32} = {} & L_{33}\, m_{N_3}\, \Big[\Big(\sqrt{m_{\nu_3}} c_1^* c_2^* c_{13} c_{23} - \sqrt{m_{\nu_2}} s_1^* c_2^* c_{12} s_{23}\Big) \\
& \Big(\sqrt{m_{\nu_3}} c_1 c_2 s_{23} + \sqrt{m_{\nu_2}} s_1 c_2 c_{12} c_{23}\Big)\Big] \\
& + L_{22}\, m_{N_2}\, \Big[\Big(\sqrt{m_{\nu_3}}(-s_1^* c_3^* - c_1^* s_2^* s_3^*) c_{23} + \sqrt{m_{\nu_2}}(s_1^* s_2^* s_3^* - c_1^* c_3^*) c_{12} s_{23}\Big) \\
& \Big(\sqrt{m_{\nu_3}}(-s_1 c_3 - c_1 s_2 s_3) s_{23} + \sqrt{m_{\nu_2}}(c_1 c_3 - s_1 s_2 s_3) c_{12}\Big)\Big] \\
& + L_{11}\, m_{N_1}\, \Big[\Big(\sqrt{m_{\nu_3}}(s_1^* s_3^* - c_1^* s_2^* c_3^*) c_{23} + \sqrt{m_{\nu_2}}(s_1^* s_2^* c_3^* + c_1^* s_3^*) c_{12} s_{23}\Big) \\
& \Big(\sqrt{m_{\nu_3}}(s_1 s_3 - c_1 s_2 c_3) s_{23} - \sqrt{m_{\nu_2}}(s_1 s_2 c_3 + c_1 s_3) c_{12} c_{23}\Big)\Big]\,,
\end{aligned}
\tag{2.10}
$$

where, $s_{ij} \equiv \sin\theta_{ij}$ and $c_{ij} \equiv \cos\theta_{ij}$, and we have already set $m_{\nu_1} = 0$ and $\theta_{13} = 0$.

The numerical predictions for $|Y_\nu^{32}|$ and $|\delta_{32}|$ as a function of θ_2 are shown in figure 1. Here we have set $M_{\rm SUSY} = M_0 = M_{1/2} = 250\,\text{GeV}$, $A_0 = 0$, $(m_{N_1}, m_{N_2}, m_{N_3}) = (10^{10}, 10^{11}, 10^{14})\,\text{GeV}$, and the light neutrino parameters are those in eq. (2.7). We see clearly that $|\delta_{32}|$ follows the same pattern as $|Y_\nu^{32}|$ (and $|Y_\nu^{33}|$) and can reach large values in the range 0.1-1 for several choices of $|\theta_2|$ and $\arg(\theta_2)$. Notice also that the predictions for $|\delta_{32}|$ corresponding to Yukawa couplings larger than about 4 are not shown, because through all this work perturbativity in all the gauge and Yukawa couplings are imposed. This is set numerically in the Spheno program by the requirement $|Y_\nu|^2/(4\pi) < 1.5$ and corresponds to a maximal predicted value of about $|\delta_{32}| < 0.4$. The corresponding predictions with respect to θ_1 are very similar to those of θ_2 and are not shown for brevity. The value of $|\delta_{32}|$ is practically independent on θ_3. For the rest of this work we will set $\theta_{1,3} = 0$ and use just θ_2 as input parameter.

The numerical predictions for $|\delta_{32}|$ as a function of the heaviest neutrino mass, m_{N_3} are shown in figure 2. $|\delta_{32}|$ values within the range 0.1-1 are obtained for large m_{N_3} values,

JHEP06(2008)079

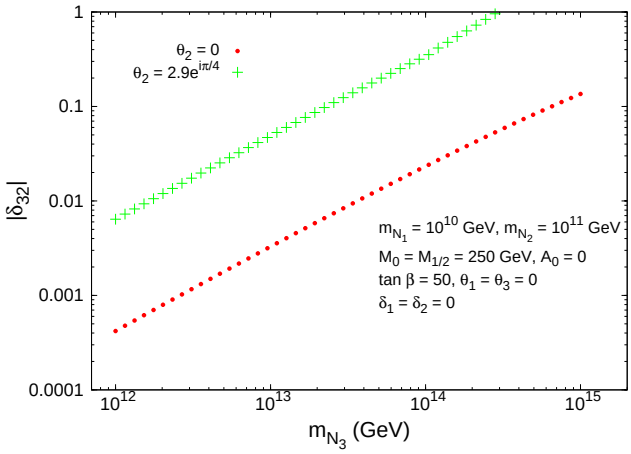

Figure 2: $|\delta_{32}|$, in the CMSSM-seesaw scenario, as a function of m_{N_3}.

say within the interval $10^{13} - 10^{15}$ GeV. Notice that the predictions enter into the above commented non-perturbative region for values larger than $m_{N_3} = 10^{14}$ GeV, and for the particular choice of $\theta_2 = 2.9\, e^{i\frac{\pi}{4}}$. Concretely, the value $|\delta_{32}| = 1$, which is interesting for later discussion and comparison with other works, corresponds to $m_{N_3} = 3 \times 10^{14}$ GeV and lies clearly in the non-perturbative region. Finally, just to mention that $|\delta_{32}|$ is not much dependent on $\tan\beta$ nor on $m_{N_{1,2}}$. The values of these two heavy neutrino masses will be set in the following to the reference values $m_{N_{1,2}} = 10^{10}, 10^{11}$ GeV.

2.2 Hadronisation of quark bilinear currents

Semileptonic decays of the tau lepton are a relatively clean scenario from the strong interaction point of view. Hadrons in the final state stem from the hadronisation of quark bilinears, namely $\overline{\psi}\,\Gamma\psi$, where ψ is a vector in the $\mathrm{SU}(3)_F$ flavour space and Γ is, in general, a matrix both in the spinor and the flavour space.

An appropriate framework to handle the procedure of hadronisation is provided by the large-N_C expansion of $\mathrm{SU}(N_C)$ QCD [45], being N_C the number of colours. In short it stays that in the $N_C \to \infty$ limit any Green function is given by meromorphic expressions provided by the tree level diagrams of a Lagrangian theory with an infinite spectrum of zero-width states. Though we do not know how to implement fully this limit, a fruitful [46] if debatable [47] approach lies in cutting the spectrum, keeping only the lightest multiplets of resonances. We will attach to this tenet as a guiding principle.

A suitable tool to realise the $1/N_C$ expansion is provided by chiral Lagrangians. In those processes where hadron resonances do not play a dynamical role, χPT [48, 49] is the appropriate scheme to describe the strong interaction of Goldstone bosons (π, K and η). This is the case, for instance, of $\tau \to \mu P$ (being P short for a pseudoscalar meson). When resonances participate in the dynamics of the process, as in $\tau \to \mu PP$, it is necessary to include them as active degrees of freedom into the Lagrangian as it is properly done in

JHEP06(2008)079

the RχT frame [37]. Hence we will make use of RχT, that naturally includes χPT, to hadronise the relevant currents that appear in the processes under study here.

We consider bilinear light quark operators coupled to external sources and added to the massles QCD Lagrangian :

$$\mathcal{L}_{\rm QCD} \,=\, \mathcal{L}^0_{\rm QCD} + \overline{q}\,[\gamma_\mu\,(v^\mu \,+\, \gamma_5\,a^\mu) \,-\, (\,s \,-\, i\,p\,\gamma_5)]\,q\,, \tag{2.11}$$

where vector ($v^\mu = v^\mu_i \lambda^i/2$), axial-vector ($a^\mu = a^\mu_i \lambda^i/2$), scalar ($s = s_i \lambda^i$) and pseudoscalar ($p = p_i \lambda^i$) fields are matrices in the flavour space, and $\mathcal{L}^0_{\rm QCD}$ is the massless QCD Lagrangian.[1] This Lagrangian density gives the QCD generating functional $\mathcal{Z}_{\rm QCD}\,[v,a,s,p]$ as

$$e^{i\,\mathcal{Z}_{\rm QCD}[v,a,s,p]} \,=\, \int [\,DG_\mu\,][\,Dq\,][\,D\overline{q}\,]\,e^{i\,\int d^4x\,\mathcal{L}_{\rm QCD}[q,\overline{q},G,v,a,s,p]}\,. \tag{2.12}$$

In order to construct the corresponding Lagrangian theory in terms of the lightest hadron modes we need to specify them. The lightest U(3) nonet of pseudoscalar mesons :

$$\begin{aligned}\phi(x) &= \sum_{a=0}^{8} \frac{\lambda_a}{\sqrt{2}}\,\varphi_a \qquad\qquad (2.13)\\ &= \begin{pmatrix} \frac{1}{\sqrt{2}}\,\pi^0 + \frac{1}{\sqrt{6}}\,\eta_8 + \frac{1}{\sqrt{3}}\eta_0 & \pi^+ & K^+ \\ \pi^- & -\frac{1}{\sqrt{2}}\,\pi^0 + \frac{1}{\sqrt{6}}\,\eta_8 + \frac{1}{\sqrt{3}}\eta_0 & K^0 \\ K^- & \bar{K}^0 & -\frac{2}{\sqrt{6}}\,\eta_8 + \frac{1}{\sqrt{3}}\eta_0 \end{pmatrix},\end{aligned}$$

is realised nonlinearly into the unitary matrix in the flavour space :

$$u(\varphi) = \exp\left[i\,\frac{\Phi}{\sqrt{2}F}\right]. \tag{2.14}$$

Hence the leading $\mathcal{O}(p^2)$ χPT SU(3)$_L \otimes$ SU(3)$_R$ chiral Lagrangian is:[2]

$$\mathcal{L}^{(2)}_\chi \,=\, \frac{F^2}{4}\,\langle u_\mu\,u^\mu \,+\, \chi_+\rangle\,, \tag{2.15}$$

where

$$\begin{aligned} u_\mu &= i[u^\dagger(\partial_\mu - ir_\mu)u - u(\partial_\mu - i\ell_\mu)u^\dagger]\,,\\ \chi_+ &= u^\dagger\chi u^\dagger + u\chi^\dagger u,\\ \chi &= 2B_0(s+ip)\ \ , \end{aligned} \tag{2.16}$$

and $\langle\ldots\rangle$ is short for a trace in the flavour space. Interactions with electroweak bosons can be accommodated through the vector $v_\mu = (r_\mu + \ell_\mu)/2$ and axial-vector $a_\mu = (r_\mu - \ell_\mu)/2$ external fields. The scalar field s incorporates explicit chiral symmetry breaking through

[1] The Gell-Mann matrices λ^i are normalised as $\langle\lambda_i\lambda_j\rangle = 2\delta_{ij}$ and the gluons are denoted here by G_μ.

[2] Notice that though we include a U(3) nonet we are not relying on the U(3)$_L \otimes$ U(3)$_R$ chiral Lagrangian [50] on grounds of predictability, as the latter introduces unknown functions.

the quark masses $s = \mathcal{M} + \cdots$ and, finally, $F \simeq F_\pi \simeq 92.4\,\mathrm{MeV}$ is the pion decay constant and $B_0 F^2 = -\langle 0|\overline{\psi}\psi|0\rangle_0$ in the chiral limit. The chiral tensor χ provides masses to the Goldstone bosons through the external scalar field, as can be seen in eq. (2.16). Indeed in the isospin limit we have :

$$\chi \,=\, 2\,B_0\,\mathcal{M} \,+ \cdots \,=\, \begin{pmatrix} m_\pi^2 & & \\ & m_\pi^2 & \\ & & 2m_K^2 - m_\pi^2 \end{pmatrix} + \,\ldots\,. \tag{2.17}$$

Hence we identify :

$$\begin{aligned} B_0\,m_u \,&=\, B_0\,m_d \,\,=\,\, \frac{1}{2}\,m_\pi^2\,, \\ B_0\,m_s \,&=\, m_K^2 - \frac{1}{2}\,m_\pi^2\,, \end{aligned} \tag{2.18}$$

that will be useful when considering the Higgs contributions. The mass eigenstates η and η' are defined from the octet η_8 and singlet η_0 states through the rotation :

$$\begin{pmatrix} \eta \\ \eta' \end{pmatrix} \,=\, \begin{pmatrix} \cos\theta & -\sin\theta \\ \sin\theta & \cos\theta \end{pmatrix} \begin{pmatrix} \eta_8 \\ \eta_0 \end{pmatrix}\,, \tag{2.19}$$

and we input[3] a value of $\theta \simeq -18^\circ$.

The hadronisation of a final state of two pseudoscalars is driven by vector and scalar resonances though the latter, because their higher masses, play a lesser role and we will not include them in the following. We will introduce the vector resonances in the antisymmetric formalism; hence the nonet of resonance fields $V_{\mu\nu}$ [37] is defined by analogy with eq. (2.13) with the same flavour structure. By demanding the chiral symmetry invariance the resonance Lagrangian reads :

$$\mathcal{L}_V \,=\, \mathcal{L}_{\rm kin}^V \,+\, \mathcal{L}_{(2)}^V\,, \tag{2.20}$$

where

$$\begin{aligned} \mathcal{L}_{\rm kin}^V \,&=\, -\frac{1}{2}\langle\,\nabla^\lambda V_{\lambda\mu}\nabla_\nu V^{\nu\mu}\,\rangle + \frac{M_V^2}{4}\,\langle\,V_{\mu\nu}V^{\mu\nu}\,\rangle\,, \\ \mathcal{L}_{(2)}^V \,&=\, \frac{F_V}{2\sqrt{2}}\langle V_{\mu\nu} f_+^{\mu\nu}\rangle + i\,\frac{G_V}{\sqrt{2}}\langle V_{\mu\nu}u^\mu u^\nu\rangle\,\,, \end{aligned} \tag{2.21}$$

and in the latter the subscript (2) indicates the chiral order of the tensor accompanying $V_{\mu\nu}$. In eq. (2.21) we have used the definitions :

$$\begin{aligned} \nabla_\mu X \,&\equiv\, \partial_\mu X + [\,\Gamma_\mu, X]\,\,, \\ \Gamma_\mu \,&=\, \frac{1}{2}\,[\,u^\dagger(\partial_\mu - ir_\mu)u + u(\partial_\mu - i\ell_\mu)u^\dagger\,]\,\,, \\ f_+^{\mu\nu} \,&=\, uF_L^{\mu\nu}u^\dagger + u^\dagger F_R^{\mu\nu}u\,, \end{aligned} \tag{2.22}$$

[3]The values of θ in the literature range between $\theta \sim -12^\circ$ up to $\theta \sim -20^\circ$ [51].

being $F^{\mu\nu}_{L,R}$ the field strength tensors associated with the external right and left fields. The couplings F_V and G_V are real.

Accordingly our RχT framework is provided by :

$$\mathcal{L}_{\mathrm{R}\chi\mathrm{T}} \,=\, \mathcal{L}^{(2)}_{\chi} \,+\, \mathcal{L}_V \,, \tag{2.23}$$

and the contribution of the low modes to the QCD functional is formally given by :

$$e^{i\,\mathcal{Z}_{\mathrm{QCD}}[v,a,s,p]}\Big|_{\text{low modes}} \,=\, \int [Du][DV]\, e^{i\,\int d^4x\,\mathcal{L}_{\mathrm{R}\chi\mathrm{T}}[u,V,v,a,s,p]}\,. \tag{2.24}$$

With this identification we can already carry out the hadronisation of the bilinear quark currents included in eq. (2.11) by taking the appropriate partial derivatives, with respect to the external auxiliary fields, of the functional action,

$$\begin{aligned}
V^i_\mu \,&=\overline{q}\,\gamma_\mu\,\frac{\lambda^i}{2}\,q \;=\; \frac{\partial\,\mathcal{L}_{\mathrm{R}\chi\mathrm{T}}}{\partial\,v^\mu_i}\Big|_{j=0}\,, & A^i_\mu \,&=\overline{q}\,\gamma_\mu\,\gamma_5\,\frac{\lambda^i}{2}\,q \;=\; \frac{\partial\,\mathcal{L}_{\mathrm{R}\chi\mathrm{T}}}{\partial\,a^\mu_i}\Big|_{j=0}\,,\\
S^i \,&=-\,\overline{q}\,\lambda^i\,q \;=\; \frac{\partial\,\mathcal{L}_{\mathrm{R}\chi\mathrm{T}}}{\partial\,s_i}\Big|_{j=0}\,, & P^i \,&=\overline{q}\,i\gamma_5\lambda^i\,q \;=\; \frac{\partial\,\mathcal{L}_{\mathrm{R}\chi\mathrm{T}}}{\partial\,p_i}\Big|_{j=0}\,,
\end{aligned} \tag{2.25}$$

where $j=0$ indicates that all external currents are set to zero. This gives :

$$\begin{aligned}
V^i_\mu \,&=\, \frac{F^2}{4}\,\langle\,\lambda^i\,\Big(u\,u_\mu\,u^\dagger\,-\,u^\dagger\,u_\mu\,u\Big)\,\rangle\,-\,\frac{F_V}{2\sqrt{2}}\,\langle\,\lambda^i\,\partial^\nu\,\Big(u^\dagger\,V_{\nu\mu}\,u\,+\,u\,V_{\nu\mu}\,u^\dagger\Big)\,\rangle\,,\\
A^i_\mu \,&=\, \frac{F^2}{4}\,\langle\,\lambda^i\,\Big(u\,u_\mu\,u^\dagger\,+\,u^\dagger\,u_\mu\,u\Big)\,\rangle\,,\\
S^i \,&=\, \frac{1}{2}\,B_0F^2\,\langle\,\lambda^i\,\Big(u^\dagger u^\dagger\,+\,uu\Big)\rangle\,,\\
P^i \,&=\, \frac{i}{2}\,B_0F^2\,\langle\,\lambda^i\,\Big(u^\dagger u^\dagger\,-\,uu\Big)\rangle\,.
\end{aligned} \tag{2.26}$$

With these expressions we are able to hadronise the final states in $\tau\to\mu PP$ and $\tau\to\mu P$ processes as we explain now :

γ contribution. The photon contribution to the decay into two pseudoscalar mesons is driven by the electromagnetic current :

$$V^{\mathrm{em}}_\mu \;=\; \sum_q^{u,d,s}\,Q_q\,\overline{q}\,\gamma_\mu\,q \;=\; V^3_\mu \,+\, \frac{1}{\sqrt{3}}\,V^8_\mu\,, \tag{2.27}$$

where Q_q is the electric charge of the q quark in units of the positron charge e. The electromagnetic form factor is then defined as :

$$\langle\,P_1(p_1)P_2(p_2)\,|\,V^{em}_\mu\,|\,0\,\rangle \;=\; (p_1-p_2)_\mu\,F_V^{P_1P_2}(s)\,, \tag{2.28}$$

where $F_V^{P_1P_2}(s)$ is steered by both $I=1$ and $I=0$ vector resonances, in particular the $\rho(770)$ that is the lightest of resonances. Due to the $q^2=0$ pole of the photon propagator

this is, by far, the dominant contribution to this hadronic final state. Hence the result is more sensitive to the construction of this form factor. Accordingly we will elaborate a more complete expression than the one provided by the vector current in eq. (2.26) though it will reduce to this one in the $N_C \to \infty$ limit, including only one multiplet of resonances and at $q^2 \ll M_\rho^2$. A proper construction of $F_V^{P_1P_2}(s)$ is given in appendix B.

Z^0 contribution. Here both vector and axial-vector currents do contribute. In terms of the quark fields these are :

$$\begin{aligned} J_\mu^Z &= V_\mu^Z + A_\mu^Z \,, \\ V_\mu^Z &= \frac{g}{2\,\cos\theta_W}\,\overline{q}\,\gamma_\mu\,\left[2\sin^2\theta_W Q - T_3^{(q)}\right]\,q \,, \\ A_\mu^Z &= \frac{g}{2\,\cos\theta_W}\,\overline{q}\,\gamma_\mu\,\gamma_5\,T_3^{(q)}\,q \,, \end{aligned} \tag{2.29}$$

with $Q = \mathrm{diag}(2,-1,-1)/3$ and $T_3^{(q)} = \mathrm{diag}(1,-1,-1)/2$ the electric charge and weak hypercharges, respectively, g is the SU(2) gauge coupling and θ_W is the weak angle.

In order to proceed to the hadronisation of these currents one has to write the currents in eq. (2.29) in terms of V_μ^i and A_μ^i defined in eq. (2.26). This gives

$$\begin{aligned} V_\mu^Z &= \frac{g}{2\,\cos\theta_W}\,\frac{F^2}{2}\,\left[2\,\sin^2\theta_W\,\langle\, Q\,\left(u u_\mu u^\dagger - u^\dagger u_\mu u\right)\rangle \,-\, \langle\, T_3^{(q)}\,\left(u u_\mu u^\dagger - u^\dagger u_\mu u\right)\rangle\right] \,, \\ A_\mu^Z &= \frac{g}{2\,\cos\theta_W}\,\frac{F^2}{2}\langle\, T_3^{(q)}\,\left(u u_\mu u^\dagger + u^\dagger u_\mu u\right)\rangle \,. \end{aligned} \tag{2.30}$$

Notice that the vector current contributes to an even number of pseudoscalar mesons while the axial-vector current provides 1,3,... mesons.

Higgs bosons contribution. Hadronisation of scalar Higgs bosons like h^0 and H^0 into two pseudoscalar mesons proceeds through the scalar current while the pseudoscalar A^0 Higgs boson hadronises through the pseudoscalar current into one pseudoscalar meson. As Higgses are rather massive the hadronisation is not so sensitive to resonances as in the case of the photon contribution. Hence we will not elaborate on scalar of pseudoscalar form factors (analogous to the vector case defined by eq. (2.28)) that, moreover, are not so well known. We will rely in the following scalar and pseudoscalar currents,

$$\begin{aligned} \overline{u}\,\Gamma\,u &= \frac{1}{2}J^3 + \frac{1}{2\sqrt{3}}J^8 + \frac{1}{\sqrt{6}}J^0 \,, \\ \overline{d}\,\Gamma\,d &= -\frac{1}{2}J^3 + \frac{1}{2\sqrt{3}}J^8 + \frac{1}{\sqrt{6}}J^0 \,, \\ \overline{s}\,\Gamma\,s &= -\frac{1}{\sqrt{3}}J^8 + \frac{1}{\sqrt{6}}J^0 \,, \end{aligned} \tag{2.31}$$

where $\Gamma = -1$ for $J^i \equiv S^i$, $\Gamma = i\gamma_5$ for $J^i \equiv P^i$ and the S^i and P^i currents are given in eq. (2.26).

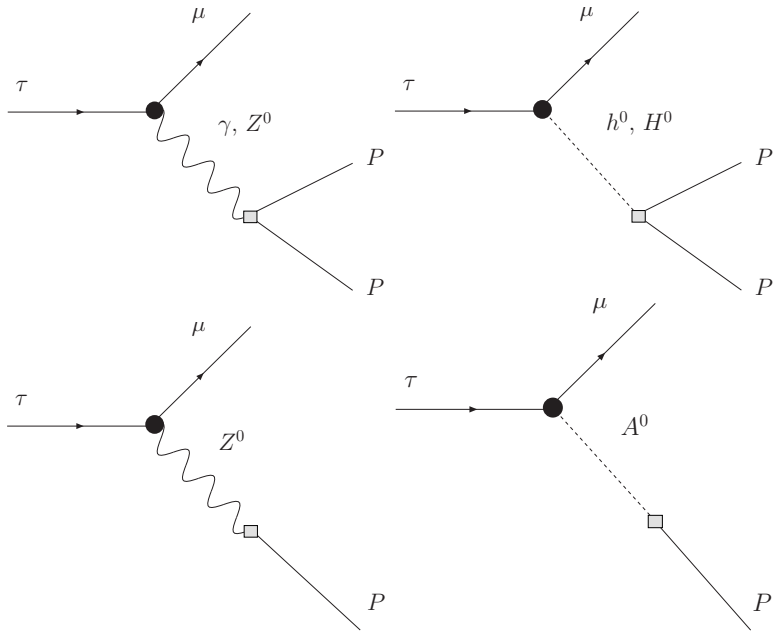

Figure 3: Contributions to LFV semileptonic τ decays into one and two pseudoscalar mesons.

3. Analytical results of the LFV semileptonic τ decays

In this section we present the analytical results of the branching ratios for the LFV semileptonic τ decays: $\tau \to \mu PP$, with $PP = \pi^+\pi^-$,$\pi^0\pi^0$, K^+K^-, $K^0\bar{K}^0$ and $\tau \to \mu P$, with $P = \pi$, η and η'. The predictions for the $\tau \to \mu\rho^0$ and $\tau \to \mu\phi$ channels, which are related to $\tau \to \mu\pi^+\pi^-$ and $\tau \to \mu K^+K^-, \mu K^0\bar{K}^0$ respectively, will also be included.

3.1 Predictions for $\tau \to \mu PP$

The semileptonic $\tau \to \mu PP$ channels can be mediated by a photon, a Z gauge boson and a CP even Higgs boson, h^0 and H^0. The various contributing diagrams are depicted in figure 3. In these diagrams, the LFV vertex is represented by a black circle and the hadronic vertex by a white box. The Z-mediated contribution is expected to be much smaller than the γ-mediated contribution due to the $\mathcal{O}(1/m_Z^2)$ suppression factor in the amplitude from the Z propagator. This has been shown to happen in the leptonic channels like $\tau \to 3\mu$, where the Z-mediated contribution to its branching ratio has been estimated to be a factor $10^{-3} - 10^{-5}$ smaller than the γ-mediated contribution, for $\tan\beta = 5 - 50$ [21]. Consequently, we have neglected here the Z contribution to the $\tau \to \mu PP$ decays. By using again this comparison with $\tau \to 3\mu$, the γ contribution to $\tau \to \mu PP$ is expected to be the dominant one, and the h^0 and H^0-mediated contributions are expected to be relevant only at large $\tan\beta$. Therefore, we have included these three γ, h^0 and H^0 contributions in the computation.

The total amplitude for the $\tau \to \mu PP$ process can be written as,

$$T = T_\gamma + T_H \,, \tag{3.1}$$

JHEP06(2008)079

where T_γ and $T_H = T_{h^0} + T_{H^0}$ are the amplitudes of the γ-mediated and H-mediated contributions respectively. First we present the result of T_γ and T_H in terms of the final state quarks, that is for $\tau \to \mu\overline{q}q$, and in terms of the corresponding τ-μ LFV form factors:

$$T_\gamma = \overline{\mu}\left[k^2\gamma_\mu\left(A_1^L P_L + A_1^R P_R\right) + im_\tau\sigma_{\mu\nu}k^\nu\left(A_2^L P_L + A_2^R P_R\right)\right]\tau \times \frac{e^2 Q_q}{k^2}\,\overline{q}\gamma^\mu q\,, \quad (3.2)$$

$$T_H = \sum_{h^0,H^0}\frac{1}{m_{H_p}^2}\Big\{H_L^{(p)}S_{L,q}^{(p)}\left[\overline{\mu}P_L\tau\right]\left[\overline{q}P_L q\right] + H_R^{(p)}S_{R,q}^{(p)}\left[\overline{\mu}P_R\tau\right]\left[\overline{q}P_R q\right] + H_L^{(p)}S_{R,q}^{(p)}\left[\overline{\mu}P_L\tau\right]\left[\overline{q}P_R q\right] + H_R^{(p)}S_{L,q}^{(p)}\left[\overline{\mu}P_R\tau\right]\left[\overline{q}P_L q\right]\Big\}\,, \quad (3.3)$$

where, k is the photon momentum, Q_q the electric charge of the quark q in units of the positron charge e, $P_{L,R} = (1 \mp \gamma_5)/2$, m_τ is the τ lepton mass, and m_{h^0}, m_{H^0} are the Higgs boson masses. Notice that the momentum of the Higgs propagators has been neglected against the Higgs boson mass. The Higgs boson couplings to quarks are correspondingly given by,

$$S_{L,u}^{(p)} = \frac{g}{2m_W}\left(\frac{-\sigma_2^{(p)*}}{\sin\beta}\right)m_u, \qquad S_{L,(d,s)}^{(p)} = \frac{g}{2m_W}\left(\frac{\sigma_1^{(p)*}}{\cos\beta}\right)m_{d,s}, \qquad S_{R,q}^{(p)} = S_{L,q}^{(p)*}, \quad (3.4)$$

where m_q is the q quark mass, m_W the W gauge boson mass, g the SU(2) gauge coupling, and

$$\sigma_1^{(p)} = \begin{pmatrix}\sin\alpha\\ -\cos\alpha\\ i\sin\beta\end{pmatrix}, \qquad \sigma_2^{(p)} = \begin{pmatrix}\cos\alpha\\ \sin\alpha\\ -i\cos\beta\end{pmatrix}. \quad (3.5)$$

The three entries for the index (p) in the previous expressions and in the following ones correspond to $H_p = h^0, H^0, A^0$, respectively. The angle α rotates, as usual, from the electroweak neutral Higgs basis to the mass eigenstate basis.

The LFV form factors $A_{1,2}^{L,R}$ in eq. (3.2) describe the effective $\gamma\tau\mu$ vertex and get contributions from the SUSY one-loop diagrams depicted in figure 16. The full results for these form factors can be found in the literature [2, 21] and are collected in appendix A.1 for completeness. Notice that we are presenting all the results in the physical mass eigenstate basis for all the particles involved. Therefore the LFV is encoded in the physical slepton and sneutrino masses and in the corresponding slepton and sneutrino rotation matrices. The later appear in the chargino-sneutrino-lepton and neutralino-slepton-lepton couplings. Similarly, the LFV form factors $H_{L,R}^{(p)}$ in eq. (3.3) describe the effective $H_p\tau\mu$ vertex and get contributions from the SUSY one-loop diagrams shown in figure 18. These set of diagrams where computed in [52] and the results are collected in appendix A.3. Again the LFV is encoded in the slepton and sneutrino masses and in the rotation matrices.

The next step is to hadronise the quark bilinears appearing in eqs. (3.2) and (3.3). For this, we proceed as explained in section 2.2. The quark bilinears in T_γ, $[\overline{q}\gamma_\mu q]$, are hadronised via the electromagnetic current in eq. (2.27) which, for the final state with two mesons $P_1(p_1)P_2(p_2)$, is then written in terms of the corresponding electromagnetic form

JHEP06(2008)079

factor, $F_V^{P_1P_2}$, by means of eq. (2.28). Thus, one gets the photon amplitude in terms of the final state hadrons:

$$T_\gamma \,=\, \frac{e^2}{k^2}\,F_V^{P_1P_2}(k^2)\,\overline{\mu}\left[k^2(\not{p}_1-\not{p}_2)\left(A_1^L P_L + A_1^R P_R\right) + 2\,i\,m_\tau\,p_1^\mu\sigma_{\mu\nu}\,p_2^\nu\left(A_2^L P_L + A_2^R P_R\right)\right]\tau. \tag{3.6}$$

The expressions of the $F_V^{P_1P_2}$ form factors for each of the final states, $P_1P_2 = \pi^+\pi^-$, K^+K^- and $K^0\bar{K}^0$ are collected in appendix B. Obviously, the $\pi^0\pi^0$ final state does not get photon-mediated contributions since γ does not couple to $\pi^0\pi^0$. Hence we set $F_V^{\pi^0\pi^0} = 0$.

The quark bilinears in T_H, $[\overline{q}P_{L,R}q]$, when hadronised in a final state of two mesons, get contributions just from scalar currents, S^i, but not from pseudoscalar currents, P^i. Then, one substitutes $[\overline{q}P_{L,R}q]$ by $[(-1/2)(-\overline{q}q)]$, where $(-\overline{q}q)$ is given in eq. (2.31), and the relevant scalar currents, S^0, S^3 and S^8, are written in terms of two mesons by using eq. (2.26). This gives:

$$\begin{aligned}
S^3 \,&=\, -B_0\left[\frac{2}{\sqrt{3}}\left(\cos\theta-\sqrt{2}\sin\theta\right)\pi^0\eta + \frac{2}{\sqrt{3}}\left(\sqrt{2}\cos\theta+\sin\theta\right)\pi^0\eta' + K^+K^- - K^0\bar{K}^0\right],\\
S^8 \,&=\, \frac{B_0}{\sqrt{3}}\left[K^+K^- + K^0\bar{K}^0 - 2\pi^+\pi^- - \pi^0\pi^0 + \left(\cos^2\theta \,+\, 2\sqrt{2}\sin\theta\cos\theta\right)\,\eta\eta\right.\\
&\qquad\qquad \left. + 2\left(\sqrt{2}\sin^2\theta + \sin\theta\cos\theta - \sqrt{2}\cos^2\theta\right)\,\eta\eta'\right],\\
S^0 \,&=\, -B_0\sqrt{\frac{2}{3}}\left[\,2\pi^+\pi^- \,+\, 2K^+K^- \,+\, 2K^0\bar{K}^0 \,+\, \pi^0\pi^0 \,+\, \eta\eta\right].
\end{aligned} \tag{3.7}$$

Thus, one gets the Higgs boson amplitude in terms of the final state hadrons:

$$T_H \,=\, \sum_{p=h^0,H^0}\overline{\mu}\left[\,c_{PP}^{(p)} \,+\, d_{PP}^{(p)}\,\gamma_5\right]\,\tau\,, \tag{3.8}$$

where

$$\begin{aligned}
c_{PP}^{(p)} \,&=\, \frac{g}{2m_W}\frac{1}{2m_{H_p}^2}\,\left(J_L^{(p)}(PP) + J_R^{(p)}(PP)\right)\left(H_R^{(p)} + H_L^{(p)}\right),\\
d_{PP}^{(p)} \,&=\, \frac{g}{2m_W}\frac{1}{2m_{H_p}^2}\,\left(J_L^{(p)}(PP) + J_R^{(p)}(PP)\right)\left(H_R^{(p)} - H_L^{(p)}\right),
\end{aligned} \tag{3.9}$$

and

$$\begin{aligned}
J_L^{(p)}(\pi^+\pi^-) \,&=\, J_L^{(p)}(\pi^0\pi^0) \,=\, \frac{1}{4}\left(\left(\frac{-\sigma_2^{(p)*}}{\sin\beta}\right)m_\pi^2 + \left(\frac{\sigma_1^{(p)*}}{\cos\beta}\right)m_\pi^2\right),\\
J_L^{(p)}(K^+K^-) \,&=\, \frac{1}{4}\left(\left(\frac{-\sigma_2^{(p)*}}{\sin\beta}\right)m_\pi^2 + \left(\frac{\sigma_1^{(p)*}}{\cos\beta}\right)(2m_K^2 - m_\pi^2)\right),\\
J_L^{(p)}(K^0\bar{K}^0) \,&=\, \frac{1}{2}\left(\frac{\sigma_1^{(p)*}}{\cos\beta}\right)m_K^2\,,\\
J_R^{(p)}(PP) \,&=\, J_L^{(p)*}(PP)\,.
\end{aligned} \tag{3.10}$$

Notice that in eq. (3.10) we have already used the relations between the quark and the meson masses of χPT given in eq. (2.18).

Finally, we get the following result for the branching ratio:

$$\mathrm{BR}(\tau \to \mu PP) \,=\, \frac{\kappa_{PP}}{64\,\pi^3\,m_\tau^2\,\Gamma_\tau} \int_{s_{\min}}^{s_{\max}} ds \int_{t_{\min}}^{t_{\max}} dt\; \frac{1}{2} \sum_{i,f} |T|^2 \,, \tag{3.11}$$

where Γ_τ is the total τ decay width, and the coefficient κ_{PP} is 1 for $PP = \pi^+\pi^-$, K^+K^-, $K^0\bar{K}^0$ and 1/2 for $PP = \pi^0\pi^0$. In addition

$$\begin{aligned}
t_{\min}^{\max} &= \frac{1}{4s}\left[\left(m_\tau^2 - m_\mu^2\right)^2 - \left(\lambda^{1/2}\left(s, m_P^2, m_P^2\right) \mp \lambda^{1/2}\left(m_\tau^2, s, m_\mu^2\right)\right)^2\right], \\
s_{\min} &= 4m_P^2\,, \\
s_{\max} &= \left(m_\tau - m_\mu\right)^2\;, \\
\lambda(x,y,z) &= (x+y-z)^2 - 4xy\,.
\end{aligned} \tag{3.12}$$

The averaged squared amplitude is,

$$\frac{1}{2}\sum_{i,f}|T|^2 \,=\, \frac{1}{8\,m_\tau}\left[g_1(s) \,+\, g_2(s)\,t \,+\, g_3(s)\,t^2\right]\,. \tag{3.13}$$

where

$$\begin{aligned}
g_1(s) &= h_0 \,+\, h_1\,s \,+\, h_2\,s^2 \,+\, h_3\,s^3\,, \\
g_2(s) &= j_1\,s \,+\, j_2\,s^2 \,+\, j_3\,s^3\,, \\
g_3(s) &= k_1\,s \,+\, k_2\,s^2\,,
\end{aligned} \tag{3.14}$$

with

$$\begin{aligned}
h_0 \,=\, & -8M_P^2 m_\tau^2\left(m_\mu^2 - m_\tau^2\right)^2\left(A_2^- A_2^{-*} + A_2^+ A_2^{+*}\right) \\
& +2\left(m_\mu + m_\tau\right)^2 c_H c_H^* \,+\, 2\left(m_\mu - m_\tau\right)^2 d_H d_H^*\,, \\
h_1 \,=\, & -8m_\tau^2\left(m_\tau m_\mu + M_P^2\right)^2 A_2^- A_2^{-*} \,-8m_\tau^2\left(m_\tau m_\mu - M_P^2\right)^2 A_2^+ A_2^{+*} \\
& +8\left(m_\mu - m_\tau\right) m_\tau \left(m_\mu + m_\tau\right)^2 M_P^2 \left(A_1^{-*} A_2^- + A_1^- A_2^{-*}\right) \\
& +8\left(m_\mu - m_\tau\right)^2 m_\tau \left(m_\mu + m_\tau\right) M_P^2 \left(A_1^{+*} A_2^+ + A_1^+ A_2^{+*}\right) \\
& -2\left(m_\mu + m_\tau\right)\left(m_\mu^2 + m_\tau^2 + 2M_P^2\right)\left(c_H A_1^{+*} + c_H^* A_1^+\right) \\
& +2m_\tau\left(m_\mu^2 + m_\tau^2 + 2M_P^2\right)\left(c_H A_2^{+*} + c_H^* A_2^+\right) \\
& -2\left(m_\mu - m_\tau\right)\left(m_\mu^2 + m_\tau^2 + 2M_P^2\right)\left(d_H A_1^{-*} + d_H^* A_1^-\right) \\
& +2m_\tau\left(m_\mu^2 + m_\tau^2 + 2M_P^2\right)\left(d_H A_2^{-*} + d_H^* A_2^-\right) \\
& -2c_H c_H^* - 2d_H d_H^*\,, \\
h_2 \,=\, & 2\left[\left(m_\mu^2 + m_\tau^2\right)^2 + 4M_P^4 + 8m_\mu m_\tau M_P^2\right] A_1^+ A_1^{+*} \\
& +2\left[\left(m_\mu^2 + m_\tau^2\right)^2 + 4M_P^4 - 8m_\mu m_\tau M_P^2\right] A_1^- A_1^{-*} \\
& +2m_\tau^2\left[\left(m_\mu - m_\tau\right)^2 + 4M_P^2\right] A_2^+ A_2^{+*} \,+\, 2m_\tau^2\left[\left(m_\mu + m_\tau\right)^2 + 4M_P^2\right] A_2^- A_2^{-*}
\end{aligned}$$

$$
\begin{aligned}
&- 2m_\tau\,(m_\mu - m_\tau)\left[(m_\mu+m_\tau)^2 + 4M_P^2\right]\left(A_1^{-*}A_2^- + A_1^- A_2^{-*}\right)\\
&- 2m_\tau\,(m_\mu + m_\tau)\left[(m_\mu-m_\tau)^2 + 4M_P^2\right]\left(A_1^{+*}A_2^+ + A_1^+ A_2^{+*}\right)\\
&+ 2\,(m_\mu+m_\tau)\left(c_H A_1^{+*} + c_H^* A_1^+\right) + 2\,(m_\mu - m_\tau)\left(d_H A_1^{-*} + d_H^* A_1^-\right)\\
&- 2m_\tau\left[c_H A_2^{+*} + c_H^* A_2^+ + d_H A_2^{-*} + d_H^* A_2^-\right],\\
h_3 =\ & -2\,(m_\mu - m_\tau)^2\ A_1^- A_1^{-*} - 2\,(m_\mu+m_\tau)^2\ A_1^+ A_1^{+*} - 2m_\tau^2\left[A_2^- A_2^{-*} + A_2^+ A_2^{+*}\right]\\
&+ 2m_\tau\,(m_\mu - m_\tau)\left[A_1^- A_2^{-*} + A_1^{-*}A_2^-\right] + 2m_\tau\,(m_\mu+m_\tau)\left[A_1^+ A_2^{+*} + A_1^{+*}A_2^+\right],\\
j_1 =\ & 8m_\tau^2\left(m_\mu^2 + m_\tau^2 + 2M_P^2\right)\left(A_2^- A_2^{-*} + A_2^+ A_2^{+*}\right)\\
&- 4m_\tau\left[c_H A_2^{+*} + c_H^* A_2^+ + d_H A_2^{-*} + d_H^* A_2^-\right]\\
&+ 4\,(m_\mu+m_\tau)\left(c_H A_1^{+*} + c_H^* A_1^+\right) + 4\,(m_\mu - m_\tau)\left(d_H A_1^{-*} + d_H^* A_1^-\right),\\
j_2 =\ & -8\left(m_\mu^2 + m_\tau^2 + 2M_P^2\right)\left[A_1^+ A_1^{+*} + A_1^- A_1^{-*}\right] - 8m_\tau^2\left[A_2^+ A_2^{+*} + A_2^- A_2^{-*}\right],\\
j_3 =\ & 8\left(A_1^- A_1^{-*} + A_1^+ A_1^{+*}\right),\\
k_1 =\ & -8m_\tau^2\left(A_2^- A_2^{-*} + A_2^+ A_2^{+*}\right),\\
k_2 =\ & 8\left(A_1^- A_1^{-*} + A_1^+ A_1^{+*}\right),
\end{aligned}
\tag{3.15}
$$

and

$$
A_i^\pm = \frac{e^2}{2\,s}\,F_V^{PP}(s)(A_i^R \pm A_i^L)\ ,\ c_H = c_{PP}^{(h^0)} + c_{PP}^{(H^0)}\ ,\ d_H = d_{PP}^{(h^0)} + d_{PP}^{(H^0)}\,. \tag{3.16}
$$

3.2 Predictions for $\tau \to \mu P$

The semileptonic $\tau \to \mu P$ channel can be mediated by a Z gauge boson and a CP odd A^0 Higgs boson, as represented in figure 3. Both contributions are included here. The total amplitude for this $\tau \to \mu P$ decay can then be written as,

$$
T = T_Z + T_{A^0}\,, \tag{3.17}
$$

where T_Z and T_{A^0} are the Z and A^0 mediated amplitudes respectively. As in the previous case, these are first evaluated in terms of the final state quarks, that is for $\tau \to \mu\overline{q}q$, and in terms of the corresponding $\tau - \mu$ LFV form factors:

$$
T_Z = \frac{1}{m_Z^2}\overline{\mu}\left[\gamma_\mu(F_L P_L + F_R P_R)\right]\tau\ .\ \overline{q}\left[\gamma^\mu\left(Z_L^{(q)}P_L + Z_R^{(q)}P_R\right)\right]q\,, \tag{3.18}
$$

$$
\begin{aligned}
T_{A^0} = \frac{1}{m_{A^0}^2}\Big\{ & H_L^{(A^0)}S_{L,q}^{(A^0)}\left[\overline{\mu}P_L\tau\right]\left[\overline{q}P_L q\right] + H_R^{(A^0)}S_{R,q}^{(A^0)}\left[\overline{\mu}P_R\tau\right]\left[\overline{q}P_R q\right]\\
& + H_L^{(A^0)}S_{R,q}^{(A^0)}\left[\overline{\mu}P_L\tau\right]\left[\overline{q}P_R q\right] + H_R^{(A^0)}S_{L,q}^{(A^0)}\left[\overline{\mu}P_R\tau\right]\left[\overline{q}P_L q\right]\Big\}\,,
\end{aligned}
\tag{3.19}
$$

where $Z_L^{(q)} = (-g/\cos\theta_W)(T_3^{(q)} - Q_q\sin^2\theta_W)$ and $Z_R^{(q)} = (g/\cos\theta_W)Q_q\sin^2\theta_W$ are the Z couplings to quarks, and $S_{L,q}^{(A^0)}$ and $S_{R,q}^{(A^0)}$ are the A^0 couplings to quarks, which are given by the third entry in eqs. (3.4) and (3.5). Notice that, as in the previous cases of h^0 and H^0, we have neglected the k^2 in the Z and A^0 propagators.

The LFV form factors $F_{L,R}$ in eq. (3.18) describe the effective $Z\tau\mu$ vertex and receive contributions from the SUSY one-loop diagrams depicted in figure 17. The results for these

form factors where found in [2] and corrected in [21]. We collect them in appendix A.2, for completeness. The LFV form factors $H_{L,R}^{(A^0)}$ in eq. (3.19) describe the effective $A^0\tau\mu$ vertex and, as in the previous $H\tau\mu$ vertices with $H = h^0, H^0$, receive contributions from the one-loop diagrams in figure 18. The corresponding results are collected in appendix A.3.

The hadronisation of the quark bilinears in T_Z proceeds by means of the vector and axial-vector currents in eq. (2.29), which in turn are written in terms of one P meson by means of eq. (2.30). This leads to:

$$V_\mu^Z = 0, \tag{3.20}$$

$$A_\mu^Z = -\frac{g}{2\cos\theta_W} F \left\{ C(\pi^0)\,\partial_\mu \pi^0 + C(\eta)\,\partial_\mu \eta + C(\eta')\,\partial_\mu \eta' \right\}, \tag{3.21}$$

where the $C(P)$ functions are given by,

$$\begin{aligned} C(\pi^0) &= 1, \\ C(\eta) &= \frac{1}{\sqrt{6}} \left(\sin\theta + \sqrt{2}\cos\theta \right), \\ C(\eta') &= \frac{1}{\sqrt{6}} \left(\sqrt{2}\sin\theta - \cos\theta \right). \end{aligned} \tag{3.22}$$

The hadronisation into one pseudoscalar meson P of the quark bilinears in T_{A^0} proceed via the pseudoscalar currents P^i. Concretely, P^0, P^3 and P^8, whose expressions in terms of one P meson can be obtained from eq. (2.26). This leads to:

$$\begin{aligned} P^3 &= 2B_0 F\, \pi^0, \\ P^8 &= 2B_0 F \left(\cos\theta\, \eta + \sin\theta\, \eta' \right), \\ P^0 &= 2B_0 F \left(-\sin\theta\, \eta + \cos\theta\, \eta' \right). \end{aligned} \tag{3.23}$$

Finally, by putting all together, we get the following result for the branching ratio:

$$\mathrm{BR}(\tau \to \mu P) = \frac{1}{4\pi} \frac{\lambda^{1/2}(m_\tau^2, m_\mu^2, m_P^2)}{m_\tau^2\, \Gamma_\tau} \frac{1}{2} \sum_{i,f} |T|^2, \tag{3.24}$$

where the $\lambda(x, y, z)$ function is defined in eq. (3.12) and again Γ_τ is the total decay width of the τ lepton. The averaged squared amplitude is given by,

$$\frac{1}{2}\sum_{i,f}|T|^2 = \frac{1}{4\,m_\tau} \sum_{k,m} \left[2m_\mu m_\tau \left(a_P^k a_P^{m\,*} - b_P^k b_P^{m\,*} \right) + (m_\tau^2 + m_\mu^2 - m_P^2) \left(a_P^k a_P^{m\,*} + b_P^k b_P^{m\,*} \right) \right], \tag{3.25}$$

with $k, m = Z, A^0$, and

$$\begin{aligned} a_P^Z &= -\frac{g}{2\cos\theta_W} \frac{F}{2} \frac{C(P)}{m_Z^2} (m_\tau - m_\mu)(F_L + F_R), \\ b_P^Z &= \frac{g}{2\cos\theta_W} \frac{F}{2} \frac{C(P)}{m_Z^2} (m_\tau + m_\mu)(F_R - F_L), \end{aligned}$$

$$a_P^{A^0} = \frac{g}{2m_W}\frac{F}{2m_{A^0}^2}\left(B_L^{(A^0)}(P) - B_R^{(A^0)}(P)\right)\left(H_L^{(A^0)} + H_R^{(A^0)}\right),$$
$$b_P^{A^0} = \frac{g}{2m_W}\frac{F}{2m_{A^0}^2}\left(B_L^{(A^0)}(P) - B_R^{(A^0)}(P)\right)\left(H_R^{(A^0)} - H_L^{(A^0)}\right). \quad (3.26)$$

The $B_{L,R}^{(A^0)}(P)$ functions are given, correspondingly, by the third entry of:

$$B_L^{(p)}(\pi) = \frac{m_\pi^2}{4}\left(\frac{-\sigma_2^{(p)*}}{\sin\beta} - \frac{\sigma_1^{(p)*}}{\cos\beta}\right),$$
$$B_L^{(p)}(\eta) = \frac{1}{4\sqrt{3}}\left[\frac{-\sigma_2^{(p)*}}{\sin\beta}m_\pi^2\left(\cos\theta - \sqrt{2}\sin\theta\right)\right. \quad (3.27)$$
$$\left. + \frac{\sigma_1^{(p)*}}{\cos\beta}\left[\left(3m_\pi^2 - 4m_K^2\right)\cos\theta - 2\sqrt{2}m_K^2\sin\theta\right]\right],$$
$$B_L^{(p)}(\eta') = \frac{1}{4\sqrt{3}}\left[\frac{-\sigma_2^{(p)*}}{\sin\beta}m_\pi^2\left(\sin\theta + \sqrt{2}\cos\theta\right)\right. \quad (3.28)$$
$$\left. + \frac{\sigma_1^{(p)*}}{\cos\beta}\left[\left(3m_\pi^2 - 4m_K^2\right)\sin\theta + 2\sqrt{2}m_K^2\cos\theta\right]\right],$$
$$B_R^{(p)}(P) = B_L^{(p)*}(P), \quad (3.29)$$

where the $\sigma_{1,2}^{(p)}$ functions are defined in eq. (3.5). Notice that in this eq. (3.29) the relations between the quark and meson masses of eq. (2.18) have been used again.

3.3 Predictions for $\tau \to \mu\rho$ and $\tau \to \mu\phi$

The $\tau \to \mu\rho^0$ decay is related to the $\tau \to \mu\pi^+\pi^-$ channel since the ρ decay proceeds mainly to $\pi^+\pi^-$. Indeed a ρ^0 is not an asymptotic state : the experiment reconstructs its structure from the two observed pions. In addition, from the chiral point of view, two pions in a $J = I = 1$ state are indistinguishable from a ρ. Therefore one has to define the branching ratio of $\tau \to \mu\rho^0$ in close relation to that of $\tau \to \mu\pi^+\pi^-$ as follows:

$$\mathrm{BR}(\tau \to \mu\rho^0) = \frac{1}{64\,\pi^3\,m_\tau^2\,\Gamma_\tau}\int_{s_{\min}}^{s_{\max}} ds \left[\int_{t_{\min}}^{t_{\max}} dt\,\frac{1}{2}\sum_{i,f}|T_\gamma|^2\right]_{\pi^+\pi^-}, \quad (3.30)$$

where T_γ is defined in eq. (3.6) and all functions and form factors involved are as those of $\tau \to \mu\pi^+\pi^-$ decay, with the exception of the integration limits in s which are now:

$$s_{\min} = M_\rho^2 - \frac{1}{2}M_\rho\Gamma_\rho\,, \qquad s_{\max} = M_\rho^2 + \frac{1}{2}M_\rho\Gamma_\rho\,. \quad (3.31)$$

Similarly, the $\tau \to \mu\phi$ decay is related to the $\tau \to \mu K^+K^-$ and $\tau \to \mu K^0\bar{K}^0$ decays since the ϕ decays proceeds mainly to K^+K^- and to $K^0\bar{K}^0$. Therefore, we define:

$$\mathrm{BR}(\tau \to \mu\phi) = \frac{1}{64\,\pi^3\,m_\tau^2\,\Gamma_\tau}\left\{\int_{s_{\min}}^{s_{\max}} ds \left[\int_{t_{\min}}^{t_{\max}} dt\,\frac{1}{2}\sum_{i,f}|T_\gamma|^2\right]_{K^+K^-}\right. \quad (3.32)$$
$$\left. + \int_{s_{\min}}^{s_{\max}} ds \left[\int_{t_{\min}}^{t_{\max}} dt\,\frac{1}{2}\sum_{i,f}|T_\gamma|^2\right]_{K^0\bar{K}^0}\right\},$$

where again T_γ is defined in eq. (3.6) and all functions and form factors involved are as those of $\tau \to \mu K^+ K^-$ and $\tau \to \mu K^0 \bar{K}^0$ correspondingly, except for the integration limits in s which are now:

$$s_{\min} = M_\phi^2 - \frac{1}{2} M_\phi \Gamma_\phi \,, \qquad s_{\max} = M_\phi^2 + \frac{1}{2} M_\phi \Gamma_\phi \,. \tag{3.33}$$

In eqs. (3.31), (3.33), $\Gamma_\rho = \Gamma_\rho(M_\rho^2)$ and $\Gamma_\phi = \Gamma_\phi(M_\phi^2)$.

4. Numerical results and discussion

In this section we present the numerical results of the LFV semileptonic $\tau \to \mu PP$ and $\tau \to \mu P$ decay rates within the constrained MSSM-seesaw scenarios described in section 2. Since our main goal is to explore if the predicted rates can or cannot reach the present experimental sensitivities we will focus mainly on choices of the input parameter values that lead to large δ_{32} and therefore to large LFV semileptonic τ decay rates. As we have seen in the previous section 2, within the scenario with hierarchical heavy neutrinos and for $\theta_{1,3} = 0$, this means large values of θ_2 and large values of m_{N_3}. On the other hand, since all these rates grow with $\tan\beta$, in the following numerical analysis we will focus mainly on large $\tan\beta$ values. In the first subsection we will present the numerical results, from our full computation of the LFV semileptonic tau decay rates and will explore the dependence with the most relevant parameters in the constrained MSSM scenarios. In the second subsection we will include a comparison between our full and some approximate results in the large $\tan\beta$ region. Moreover, we will also analyse to what extent the Higgs dominance hypothesis holds for these LFV semileptonic τ decays and compare our predictions with other results in the literature. We will conclude this section by showing that for some particular choices of the input parameters, the rates for some channels indeed reach the present experimental sensitivity.

4.1 LFV semileptonic tau decay rates

Firstly, we present the results for the simplest case of $\theta_2 = 0$ and study the relative importance of the various contributions to the decay rates that have been presented in the previous section. Then we explore the increase in the rates for larger values of θ_2. Since we are setting in the whole numerical analysis $A_0 = 0$ and sign $(\mu) = +1$, the relevant SUSY parameter will be $M_{\rm SUSY} = M_0 = M_{1/2}$. In the study of the behaviour of the rates with $M_{\rm SUSY}$ we pay special attention to the decoupling or non-decoupling behaviour of the SUSY particles at large $M_{\rm SUSY}$.

In figure 4 we display the prediction of $\mathrm{BR}(\tau \to \mu PP)$, with $PP = \pi^+\pi^-$, K^+K^-, $K^0\bar{K}^0$, $\pi^0\pi^0$, as a function of $M_{\rm SUSY}$ and for the particular choice of $\theta_i = 0$ $(i = 1, 2, 3)$. We consider both CMSSM (left panel) and NUHM (right panel) scenarios. We set here $\tan\beta = 50$ and our "reference" values of $m_{N_{1,2,3}} = (10^{10}, 10^{11}, 10^{14})\,\mathrm{GeV}$. For the NUHM case we set in addition $\delta_1 = -1.8$ and $\delta_2 = 0$, which have been shown in [24] to lead to low Higgs boson mass values. Concretely, for $\theta_i = 0$ and $250\,\mathrm{GeV} < M_{\rm SUSY} < 900\,\mathrm{GeV}$ the predicted masses are within the range $110\,\mathrm{GeV} < m_{A^0}, m_{H^0} < 180\,\mathrm{GeV}$, which are indeed very close to their present experimental bounds.

JHEP06(2008)079

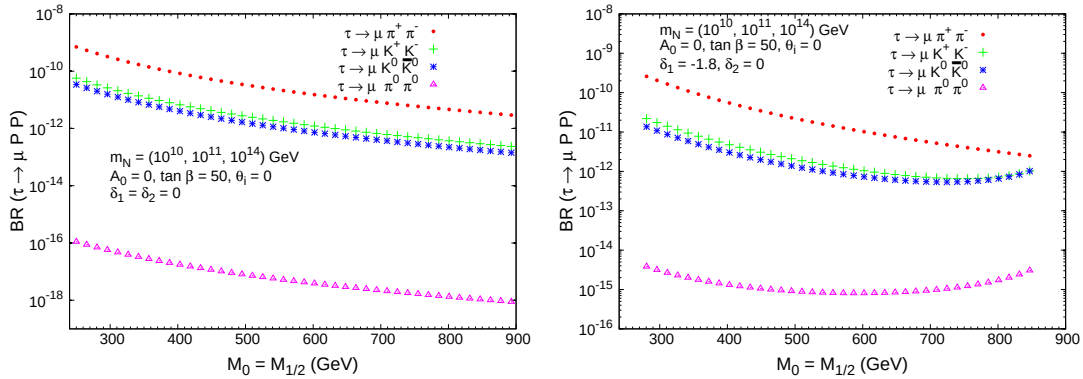

Figure 4: BR($\tau \to \mu PP$) for $PP = \pi^+\pi^-, K^+K^-, K^0\bar{K}^0, \pi^0\pi^0$ as a function of $M_{\rm SUSY} = M_0 = M_{1/2}$ in the contrained MSSM-seesaw scenarios: CMSSM (left panel) and NUHM (right panel).

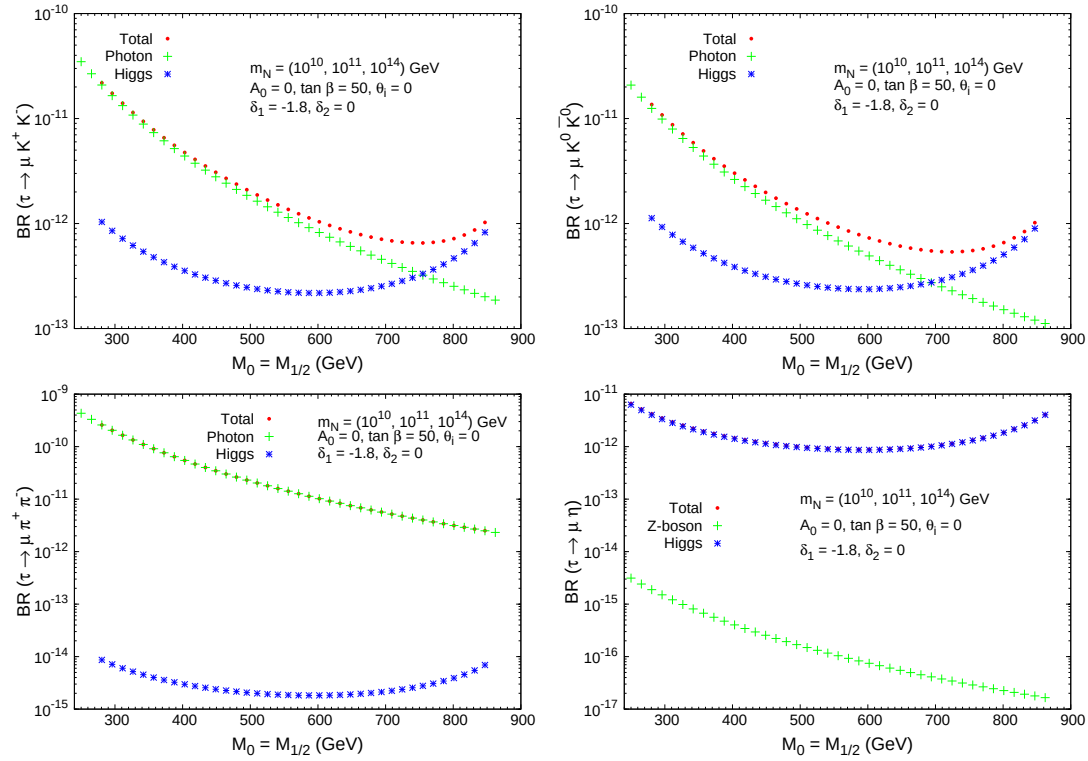

Figure 5: Rates of the various contributions to BR($\tau \to \mu K^+K^-$) (upper left panel), BR($\tau \to \mu K^0\bar{K}^0$) (upper right panel), BR($\tau \to \mu\pi^+\pi^-$) (lower left panel) and BR($\tau \to \mu\eta$) (lower right panel) as a function of $M_{\rm SUSY} = M_0 = M_{1/2}$ in the NUHM scenario.

The first obvious conclusion from figure 4 is that the rates of the different channels exhibit the following hierarchy, BR($\tau \to \mu\pi^+\pi^-$) > BR($\tau \to \mu K^+K^-$) $\gtrsim$ BR($\tau \to \mu K^0\bar{K}^0$) $\gg$ BR($\tau \to \mu\pi^0\pi^0$). This hierarchy can be understood in terms of the dominant electromagnetic contribution and the relative phase space suppression. We also see that the

JHEP06(2008)079

decoupling behaviour for large $M_{\rm SUSY}$ is clearly manifest in the universal case, where all the rates decrease as $M_{\rm SUSY}$ grows. In contrast, it turns out that, in the NUHM case, the decoupling behaviour is only manifest in the $\tau \to \mu\pi^+\pi^-$ channel, whereas the $\tau \to \mu K^+K^-$, $\tau \to \mu K^0\bar{K}^0$ and $\tau \to \mu\pi^0\pi^0$ rates do not decrease with $M_{\rm SUSY}$ in the large $M_{\rm SUSY}$ region. This behaviour can be better comprehended by analysing separately the different contributions to these channels, as shown in figure 5.

The results displayed in Fig 5 for the $\tau \to \mu\pi^+\pi^-$ channel show the dominance of the photon-mediated contribution in this case, which is in fact indistinguishable from the total rate in this plot, for all the explored parameter values. The Higgs-mediated contribution is subdominant by far due to the highly suppressed couplings of the Higgs to the light u and d quarks, which after the hadronisation of the corresponding quark bilinears result in $H\pi^+\pi^-$ couplings proportional to m_π^2 (see eq. (3.10)). This plot also exhibits the non-decoupling behaviour of the SUSY particles in the Higgs-mediated contribution. The particular pattern of this contribution as a function of $M_{\rm SUSY}$ is a consequence of two facts. First, the well known constant behaviour with $M_{\rm SUSY}$ of the LFV $H\tau\mu$ form factor at large $M_{\rm SUSY}$. Second, the encountered Higgs mass behaviour with $M_{\rm SUSY}$, analysed in [24], which, for this choice of $\delta_{1,2}$ and for the studied $M_{\rm SUSY}$ interval, first grows softly, reaches a maximum and then decreases softly.

The $\tau \to \mu\pi^0\pi^0$ channel is only mediated by the Higgs bosons and a similar suppression of $H\pi^0\pi^0$ couplings as in the $H\pi^+\pi^-$ case occurs, leading to very low predicted rates. These low rates and the non-decoupling behaviour of this channel can be clearly seen in figure 4.

The results for the $\tau \to \mu K^+K^-$ channel that are depicted in Fig 5 are interesting because the photon- and the Higgs-mediated contributions compete in this decay. In fact the Higgs-mediated contribution can equalise, or even exceed that of the photon, dominating the total rate in the large $M_{\rm SUSY}$ region. Both photon- and Higgs-mediated contributions are similar around $M_{\rm SUSY} = 750\,\text{GeV}$. The reason for this larger Higgs contributions than in the previously studied $\pi\pi$ case is because of the larger Higgs couplings to the strange quarks which result in HKK couplings proportional to m_K^2 (see eq. (3.10)).

The results for the $\tau \to \mu K^0\bar{K}^0$ channel in Fig 5 are very similar to those for $\tau \to \mu K^+K^-$. One difference is the point where the Higgs-mediated contribution crosses the photon one, which for $\tau \to \mu K^0\bar{K}^0$ is around $M_{\rm SUSY} = 700\,\text{GeV}$. Another interesting difference is that this rate is always slightly smaller than $\tau \to \mu K^+K^-$ due to the fact that the photon-mediated contribution to $\tau \to \mu K^0\bar{K}^0$ occurs just by the meson resonances, whereas the $\tau \to \mu K^+K^-$ channel can also be mediated via pure electromagnetic interaction. This difference is clearly summarised in the several contributions to the $F_V^{K^+K^-}$ and $F_V^{K^0\bar{K}^0}$ form factors in eq. (B.3) of appendix B.

The predictions of $\text{BR}(\tau \to \mu P)$, with P being here a pseudoscalar meson π, η, η' or a vector resonance ρ, ϕ, as a function of $M_{\rm SUSY}$ are displayed in figure 6. We also consider CMSSM (left panel) and NUHM (right panel) scenarios. In the universal case we find the following hierarchy, $\text{BR}(\tau \to \mu\rho) > \text{BR}(\tau \to \mu\phi) > \text{BR}(\tau \to \mu\eta') \gtrsim \text{BR}(\tau \to \mu\eta) > \text{BR}(\tau \to \mu\pi)$. We obtain again the expected decoupling behaviour for large $M_{\rm SUSY}$ in this universal scenario, while in the NUHM scenario the non-decoupling behaviour is clearly manifest for $\tau \to \mu\eta$, $\tau \to \mu\eta'$ and $\tau \to \mu\pi$. The $\tau \to \mu\rho$ rates in the NUHM scenario are

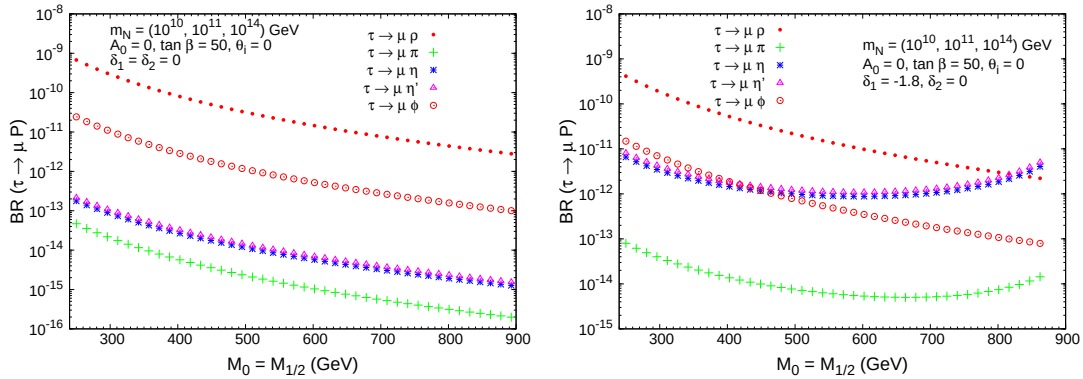

Figure 6: BR($\tau \to \mu P$) for $P = \pi, \eta, \eta', \rho, \phi$ as a function of $M_{\rm SUSY} = M_0 = M_{1/2}$ in the contrained MSSM-seesaw scenarios: CMSSM (left panel) and NUHM (right panel).

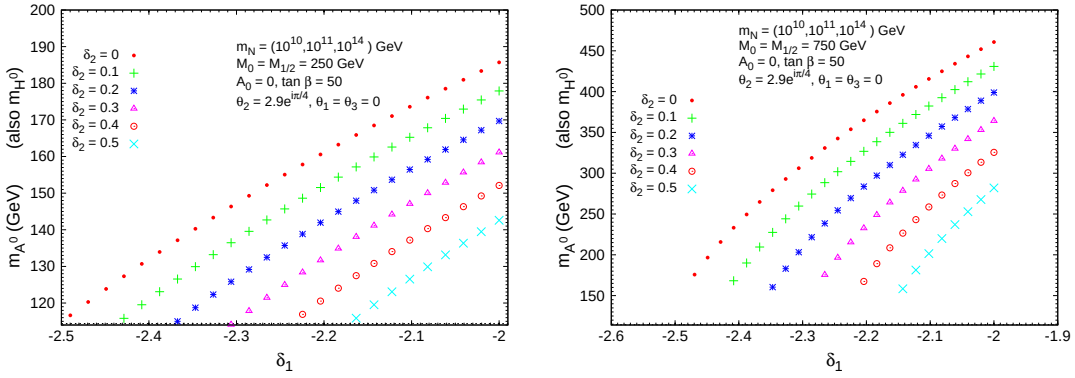

Figure 7: Light m_{A^0} predictions as a function of non-universal parameters δ_1 and δ_2 in the NUHM scenario. The predictions for m_{H^0} are indistinguisable from those of m_{A^0} in this figure.

the largest ones, except in the large $M_{\rm SUSY}$ region, where $\tau \to \mu\eta$ and $\tau \to \mu\eta'$ rates exceed them. These two channels are by far dominated by the Higgs-mediated contributions in the full $M_{\rm SUSY}$ explored interval, as can be seen for the η case in Fig 5. The reason for this Higgs dominance is because of the large Higgs couplings to the strange components of the η and η' mesons, which result in large $A^0 - \eta$ and $A^0 - \eta'$ "mixings" proportional to m_K^2 as explicitely given in eq. (3.29).

One of the most important outcomes from the previous analysis, corresponding to the $\theta_i = 0$ choice, is that for both scenarios and for the chosen input parameters, the predicted rates for both $\tau \to \mu PP$ and $\tau \to \mu P$ channels do no reach their corresponding experimental bounds, and even in the best cases of $\tau \to \mu\pi^+\pi^-$ and $\tau \to \mu\rho$ they are still two orders of magnitude below their present experimental sensitivities. In the following, we will therefore focus on larger values of θ_2.

In order to reach the larger rates as possible in the $\theta_i \neq 0$ case, one needs to explore first the optimal values of δ_1 and δ_2 which lead to light Higgs bosons. We summarise the

JHEP06(2008)079

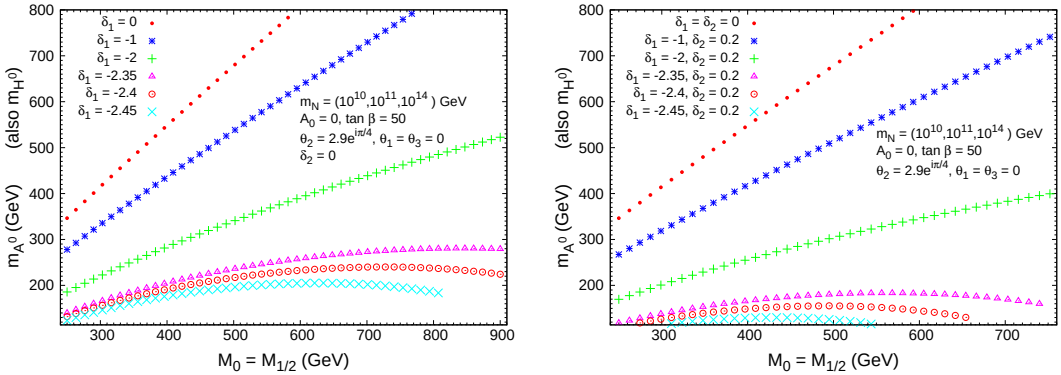

Figure 8: Light m_{A^0} predictions as a function of $M_{\rm SUSY} = M_0 = M_{1/2}$ in the NUHM scenario. The predictions for m_{H^0} are indistinguisable from those of m_{A^0} in this figure. The predictions for the CMSSM scenario ($\delta_1 = \delta_2 = 0$) are also included for comparison.

predictions for the relevant Higgs boson mass, m_{A^0} (and m_{H^0}), as a function of δ_1 and δ_2 in figure 7 for the extreme value of $\theta_2 = 2.9e^{i\pi/4}$. The reason for this particular choice of θ_2 is due to the fact that it leads to the maximum value of $|\delta_{32}|$ which is compatible with our hypothesis of perturbativity, as shown in figure 1 and discussed in section 2. We have chosen here $\tan\beta = 50$ and two representative values of $M_{\rm SUSY} = 250$ and $750\,\text{GeV}$ for moderate and heavy SUSY spectra, respectively. The other parameters are set to the values of $m_{N_i} = (10^{10}, 10^{11}, 10^{14})\,\text{GeV}$, $\theta_1 = \theta_3 = 0$, $A_0 = 0$ and $\text{sign}(\mu) = +1$. To ensure that our results are indeed experimentally viable, we have included in this, and in the following figures, only the solutions where the three neutral Higgs boson masses are above the experimental bound for the lightest MSSM Higgs boson, which at present is $110\,\text{GeV}$ for $\tan\beta > 5$ (99.7% C.L.) [7]. The most interesting solutions with important phenomenological implications are found for negative δ_1 within the range $(-3, -2)$ and very small and positive δ_2, the choices selected for figure 7. In this figure, for all the explored values of δ_1 and δ_2, we find a value of m_{A^0} that is significantly smaller than what one would encounter in the universal case (here represented by the choice $\delta_1 = \delta_2 = 0$). This is truly remarkable in the case of large soft breaking masses, as can be seen, for instance, in the panel with $M_{\rm SUSY} = 750\,\text{GeV}$, where low values of $m_{A^0} \sim 150\,\text{GeV}$ are still found.

The behaviour of the predicted m_{A^0} as a function of $M_{\rm SUSY}$ is depicted in figure 8. Here the specific values of $\delta_1 = \{-2.45, -2.4, -2.35, -2, -1, 0\}$ and $\delta_2 = 0, 0.2$ have been considered. This figure illustrates again the interesting departure in NUHM scenarios from the linear behaviour of m_{A^0} with $M_{\rm SUSY}$, which is generic in the universal case ($\delta_1 = \delta_2 = 0$). The same pattern with $M_{\rm SUSY}$ was also found for the $\theta_i = 0$ case in [24], but obviously for different choices of δ_1 and δ_2.

The corresponding predictions for $\theta_2 = 2.9e^{i\pi/4}$ of the nine LFV semileptonic τ decays studied in this work as a function of $M_{\rm SUSY}$ are shown in figure 9. In this case, we work with $\delta_1 = -2.4$ and $\delta_2 = 0.2$, that drive us to Higgs boson masses around $150\,\text{GeV}$ even for heavy SUSY spectra, as can be seen in figures 7 and 8. In this figure 9 we can see that,

JHEP06(2008)079

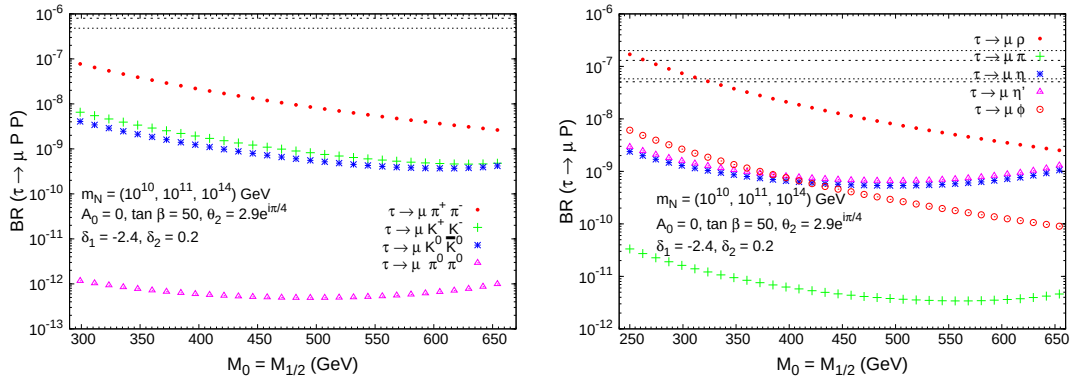

Figure 9: Predictions of BR($\tau \to \mu PP$) and BR($\tau \to \mu P$) as a function of $M_{\rm SUSY}$ in the NUHM scenario for a large $\tau - \mu$ mixing driven by $\theta_2 = 2.9e^{i\pi/4}$. The horizontal lines are the present experimental bounds given in table 1.

compared to predictions in figures 4 and 6, the new choice of θ_2 increase all the rates about two orders of magnitude. All the rates exhibit the same hierarchy as in the previous plots, being BR($\tau \to \mu\pi^+\pi^-$) and BR($\tau \to \mu\rho$) the largest ones. Indeed, the predictions of these two latter channels reach their present experimental sensitivities at the low $M_{\rm SUSY}$ region, below 200 GeV and 250 GeV respectively, for this particular choice of input parameters.

4.2 Comparison between the full and approximate results

It is interesting and useful to provide simple formulas that can approximate reasonably well our full predictions. The most popular approximation when predicting LFV rates is to work with expressions that are valid only in the large $\tan\beta$ region. The justification for this is obvious since all these LFV rates are known to grow with $\tan\beta$. It is specially important in scenarios where the LFV rates are dominated by the Higgs mediated diagrams, since these latter grow much faster with $\tan\beta$ than the photon or Z boson mediated ones. Accordingly, we will pay more attention to the semileptonic $\tau \to \mu P$ and $\tau \to \mu PP$ channels that can be dominated by the Higgs bosons and whose present experimental sensitivities are the best ones. This leads us mainly to the $\tau \to \mu\eta$ and $\tau \to \mu K^+K^-$ channels. The other approximation which is used frequently in the literature, due to its simplicity, is the mass insertion approximation, where the tau-muon LFV is encoded in the dimesionless parameter δ_{32}, already introduced in section 2, and whose expression in the LLog approximation is given in eqs. (2.9) and (2.10).

We start by considering the large $\tan\beta$ limit of the tau-muon-Higgs form factors that are the relevant ones for the LFV Higgs-mediated processes. The full one-loop Higgs form factors were computed in [52] (see also [21]) and are collected in appendix A.2. At large $\tan\beta$, H_L dominates H_R by about a factor m_τ/m_μ. Moreover, $H_L^{A^0}$ and $H_L^{H^0}$ are by far the largest form factors in this limit, and one can safely neglect $H_L^{h^0}$. More specifically, by using the mass insertion approximation, their chargino and neutralino contributions in the

JHEP06(2008)079

large $\tan\beta$ limit give, correspondingly, the following results [52],

$$H_{L,c}^{(A^0)} \;=\; iH_{L,c}^{(H^0)} \;=\; i\,\frac{g^3}{16\pi^2}\,\frac{m_\tau}{12m_W}\,\delta_{32}\,\tan^2\beta\,, \tag{4.1}$$

$$H_{L,n}^{(A^0)} \;=\; iH_{L,n}^{(H^0)} \;=\; i\,\frac{g^3}{16\pi^2}\,\frac{m_\tau}{24m_W}\,(1-3\tan^2\theta_W)\,\delta_{32}\,\tan^2\beta\,. \tag{4.2}$$

One can further verify that H_c dominates H_n by about a factor 20, so that in the following we will take $H_L \simeq H_{L,c}$.

On the other hand, we also consider the large $\tan\beta$ limit of the functions that define the Higgs couplings to one meson, $B(P)$ in eq. (3.29), and to two mesons, $J(PP)$ in eq. (3.10). It leads to the following results:

$$\begin{aligned}
B_L^{(A^0)}(\eta) &= -B_R^{(A^0)}(\eta) \;=\; -i\frac{1}{4\sqrt{3}}\tan\beta\left[(3m_\pi^2-4m_K^2)\cos\theta-2\sqrt{2}m_K^2\sin\theta\right]\,,\\
B_L^{(A^0)}(\eta') &= -B_R^{(A^0)}(\eta') \;=\; -i\frac{1}{4\sqrt{3}}\tan\beta\left[(3m_\pi^2-4m_K^2)\sin\theta+2\sqrt{2}m_K^2\cos\theta\right]\,,\\
B_L^{(A^0)}(\pi) &= -B_R^{(A^0)}(\pi) \;=\; i\frac{1}{4}\tan\beta\,m_\pi^2\,,\\
J_L^{(H^0)}(K^+K^-) &= J_R^{(H^0)}(K^+K^-) \;=\; -\frac{1}{4}\tan\beta\,(2m_K^2-m_\pi^2)\,,\\
J_L^{(H^0)}(K^0\bar{K}^0) &= J_R^{(H^0)}(K^0\bar{K}^0) \;=\; -\frac{1}{2}\tan\beta\,m_\pi^2\,,\\
J_L^{(H^0)}(\pi^+\pi^-) &= J_R^{(H^0)}(\pi^+\pi^-) \;=\; J_L^{(H^0)}(\pi^0\pi^0) \;=\; J_R^{(H^0)}(\pi^0\pi^0) \;=\; -\frac{1}{4}\tan\beta\,m_\pi^2\,.
\end{aligned} \tag{4.3}$$

By using the above sequence of approximations and by neglecting the muon mass, we finally get the following simple results,

$$\begin{aligned}
\mathrm{BR}(\tau\to\mu\eta)_{H_{\rm approx}} &= \frac{1}{8\pi m_\tau^3}\left(m_\tau^2-m_\eta^2\right)^2\left|\frac{g}{2m_W}\,\frac{F}{m_{A^0}^2}\,B_L^{(A^0)}(\eta)\,H_{L,c}^{(A^0)}\right|^2\frac{1}{\Gamma_\tau}\\
&= 1.2\times10^{-7}\,|\delta_{32}|^2\left(\frac{100}{m_{A^0}(\mathrm{GeV})}\right)^4\left(\frac{\tan\beta}{60}\right)^6\,,
\end{aligned} \tag{4.4}$$

and

$$\begin{aligned}
\mathrm{BR}(\tau\to\mu K^+K^-)_{H_{\rm approx}} &= \frac{1}{128m_\tau\pi^3}\left|\frac{g}{2m_W}\frac{1}{m_{H^0}^2}J_L^{(H^0)}(K^+K^-)H_{L,c}^{(H^0)}\right|^2\frac{1}{\Gamma_\tau}\\
&\qquad\times\int_{s_{\rm min}}^{s_{\rm max}}ds\,(t_{\rm max}-t_{\rm min})\left(1-\frac{s}{m_\tau^2}\right)\\
&= 2.8\times10^{-8}\,|\delta_{32}|^2\left(\frac{100}{m_{H^0}(\mathrm{GeV})}\right)^4\left(\frac{\tan\beta}{60}\right)^6\,,
\end{aligned} \tag{4.5}$$

where $s_{\rm max}$, $s_{\rm min}$, $t_{\rm max}$ and $t_{\rm min}$ are given in eq. (3.12). The results for the other channels can be similarly obtained by using the corresponding $B(P)$ or $J(PP)$ functions and the corresponding meson masses (with an additional 1/2 factor in the case of $BR(\tau\to\mu\pi^0\pi^0)$

JHEP06(2008)079

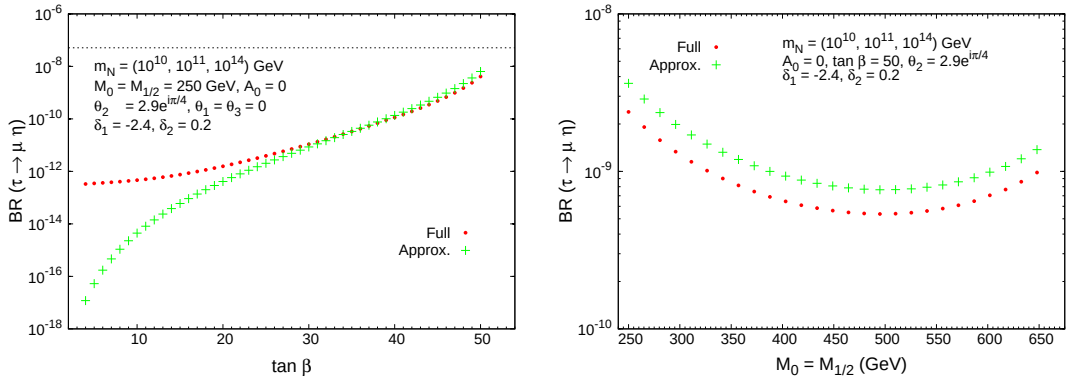

Figure 10: Comparison between the predicted rates of $\mathrm{BR}(\tau \to \mu\eta)$ in the NUHM from our full 1-loop computation and from the approximate result of eq. (4.4) as a function of $\tan\beta$ (left panel) and $M_{\rm SUSY} = M_0 = M_{1/2}$ (right panel). The horizontal lines are the present experimental bounds given in table 1.

to account for identical final state particles). We get,

$$\mathrm{BR}(\tau \to \mu\eta')_{H_{\rm approx}} = 1.5 \times 10^{-7} \, |\delta_{32}|^2 \left(\frac{100}{m_{A^0}(\mathrm{GeV})}\right)^4 \left(\frac{\tan\beta}{60}\right)^6 , \tag{4.6}$$

$$\mathrm{BR}(\tau \to \mu\pi)_{H_{\rm approx}} = 3.6 \times 10^{-10} \, |\delta_{32}|^2 \left(\frac{100}{m_{A^0}(\mathrm{GeV})}\right)^4 \left(\frac{\tan\beta}{60}\right)^6 , \tag{4.7}$$

$$\mathrm{BR}(\tau \to \mu K^0 \bar{K}^0)_{H_{\rm approx}} = 3.0 \times 10^{-8} \, |\delta_{32}|^2 \left(\frac{100}{m_{H^0}(\mathrm{GeV})}\right)^4 \left(\frac{\tan\beta}{60}\right)^6 , \tag{4.8}$$

$$\mathrm{BR}(\tau \to \mu\pi^+\pi^-)_{H_{\rm approx}} = 2.6 \times 10^{-10} \, |\delta_{32}|^2 \left(\frac{100}{m_{H^0}(\mathrm{GeV})}\right)^4 \left(\frac{\tan\beta}{60}\right)^6 , \tag{4.9}$$

$$\mathrm{BR}(\tau \to \mu\pi^0\pi^0)_{H_{\rm approx}} = 1.3 \times 10^{-10} \, |\delta_{32}|^2 \left(\frac{100}{m_{H^0}(\mathrm{GeV})}\right)^4 \left(\frac{\tan\beta}{60}\right)^6 . \tag{4.10}$$

In all the above approximate results of the LFV semileptonic tau decay rates we see explicitely the strong dependence with both $\tan\beta$ and the corresponding Higgs boson mass, being $(\tan\beta)^6$ and $(1/m_H)^4$, respectively, which are characteristic of the Higgs mediated processes.

Regarding the comparison with other works, first, we notice that our numerical prediction for $\mathrm{BR}(\tau \to \mu\eta)$ in eq. (4.4) does not agree with the original estimate in [31] that gives a decay rate a factor 7 larger than ours. We believe that the discrepancy comes from our different approaches to describe the hadronisation of quark bilinears. Our numerical result is closer to that in [32] whose prediction is larger than ours in a factor of 2. Notice, that the comparison with this latter work must be done by switching off the bottom-loop induced contributions and the higher order loop-effects enhanced by $\tan\beta$ factors which were taken into account in [32] but we are not including here. This means setting their ξ_q parameters to $\xi_b = 0$ and $\xi_s = 1$ in their formulas. We believe that this small discrepancy is mainly due to the different approaches for hadronisation. In particular, they neglect the

JHEP06(2008)079

$m_{u,d}$ masses whereas we are taking into account chiral symmetry breaking effects via the explicit m_π^2 and m_K^2 dependences, which are well determined in the χPT approach. On the other hand, our prediction for $\mathrm{BR}(\tau \to \mu\eta')$ is slightly above $\mathrm{BR}(\tau \to \mu\eta)$, due basically to the larger Higgs coupling to η', $|B_L(\eta')^{(A_0)}| > |B_L(\eta)^{(A_0)}|$. The prediction in [32] of $\mathrm{BR}(\tau \to \mu\eta')$ is, however, a factor 100 smaller than ours. The prediction for $\mathrm{BR}(\tau \to \mu\pi)$ here and in [32] agree within a factor of 2. Finally, the prediction for $\mathrm{BR}(\tau \to \mu K^+K^-)$ in [34] is larger than our result in about a factor 50.

The goodness of the above approximate result for $\tau \to \mu\eta$ in eq. (4.4) can be seen in figure 10, where it is compared with the full result as a function of $\tan\beta$ and $M_{\rm SUSY}$. It is clear that, for $\tan\beta$ values larger than about 30 the approximation is quite good, providing rates that are at most a factor of 2 above the full predictions. Moreover, the behaviour with $\tan\beta$ of the full result at this region is well described by the $(\tan\beta)^6$ behaviour of the approximate one. Regarding the behaviour with $M_{\rm SUSY}$, we see again that the approximate and full results differ by less than a factor of 2 and they both follow the same pattern. The displayed dependence with $M_{\rm SUSY}$ can be easily understood from the dependence of m_{A^0} with this parameter, as was shown in figure 8. For the studied range in this plot, $250 < M_{\rm SUSY}\,(\mathrm{GeV}) < 650$, this leads to a relatively small variation in the rates of about $BR_{\rm max}/BR_{\rm min} \sim 5$.

The Higgs dominance approach, however, is not so good for other LFV tau decay channels. In particular, it is clearly not a good approximation for $\tau \to 3\mu$ because, in this case, there are other contributions from γ-mediated, Z-mediated and box diagrams that enter into the full computation [2, 21]. In the NUHM scenarios that are considered here with small Higgs masses, one may guess that the Higgs mediated contribution could dominate the rates at large $\tan\beta$, but it is not so as will be shown next. By performing a similar analysis as we have done before, that is, by using the tau-muon-Higgs form factors in eq. 4.1 and plugging it into the exact formula for the Higgs-contribution [21], we get in the large $\tan\beta$ limit,

$$\mathrm{BR}(\tau \to 3\mu)_{H_{\rm approx}} = \frac{G_F^2}{2048\pi^3}\frac{m_\tau^7 m_\mu^2}{\Gamma_\tau}\left(\frac{1}{m_{H^0}^4}+\frac{1}{m_{A^0}^4}+\frac{2}{3m_{H^0}^2 m_{A^0}^2}\right)\left|\frac{g^2\delta_{32}}{96\pi^2}\right|^2 (\tan\beta)^6 \quad (4.11)$$

$$= 1.2\times 10^{-7}\,|\delta_{32}|^2\left(\frac{100}{m_{A^0}(\mathrm{GeV})}\right)^4\left(\frac{\tan\beta}{60}\right)^6, \quad (4.12)$$

which is in good agreement with the original result in [18] and also with posterior estimates [19, 32].

The comparison between the full (i.e. including one-loop SUSY diagrams mediated by γ, Z, h_0, H_0, A_0 and box diagrams which are taken from [21]) and the approximate numerical results for this channel is shown in figure 11. We see that the formula in eq. (4.11) predicts rates that are about a factor of 2 larger than the exact Higgs-mediated contribution. Therefore, for large $\tan\beta$ values, it provides a good estimate of the Higgs contribution. However, the total rates are much larger than the Higgs contribution, since the photon-mediated diagrams give by far the dominant contribution in this channel. For instance, we see in figure 11 that the total and Higgs rates differ in about two orders of magnitude for $M_{\rm SUSY} \sim 250\,\mathrm{GeV}$ and in more than a factor 5 for $M_{\rm SUSY} \sim 750\,\mathrm{GeV}$. It

JHEP06(2008)079

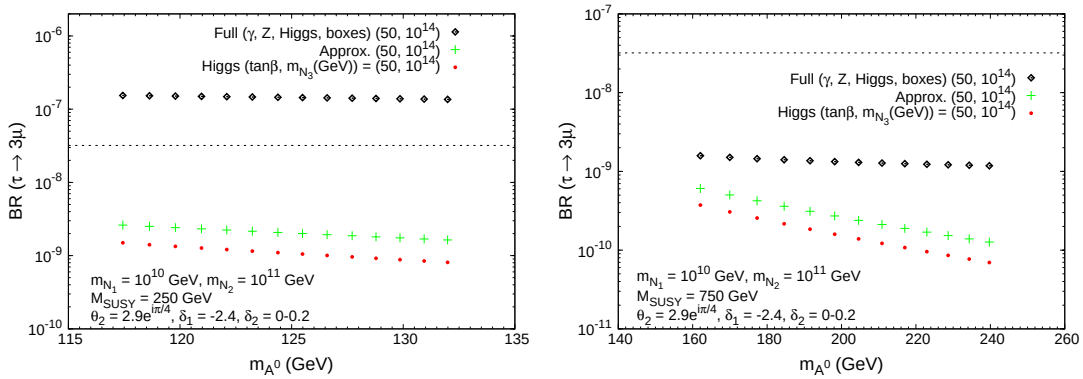

Figure 11: Comparison between the full and approximate results for $\tau \to 3\mu$ as a function of m_{A^0} in the NUHM scenario, for $M_{\rm SUSY} = M_0 = M_{1/2} = 250\,\text{GeV}$ (left panel) and for $M_{\rm SUSY} = M_0 = M_{1/2} = 750\,\text{GeV}$ (right panel). The dashed horizontal line is the present experimental upper bound [16].

is remarkable that, in this channel, the photon dominance holds largely even in scenarios with very heavy SUSY spectra, as for $M_{\rm SUSY} \sim 750\,\text{GeV}$, and Higgs bosons as light as $m_H = 160\,\text{GeV}$. Therefore, the total rates for this channel can be better approximated by the simplified formula of the photon-mediated contribution,

$$\begin{aligned}\text{BR}(\tau \to 3\mu)_{\gamma_{\rm approx}} &= \frac{\alpha}{3\pi}\left(\log\frac{m_\tau^2}{m_\mu^2} - \frac{11}{4}\right)\text{BR}(\tau \to \mu\gamma) \\ &= 2.3 \times 10^{-3}\ \text{BR}(\tau \to \mu\gamma) \\ &= 3.4 \times 10^{-5}\,|\delta_{32}|^2 \left(\frac{100}{M_{\rm SUSY}(\text{GeV})}\right)^4 \left(\frac{\tan\beta}{60}\right)^2, \end{aligned} \tag{4.13}$$

where the last line has been obtained by using the result of $\text{BR}(\tau \to \mu\gamma)$ in the mass insertion approximation for equal SUSY mass scales and in the large $\tan\beta$ limit. It is also interesting to compare this estimate with the present experimental upper bound for this channel which is 3.2×10^{-8} [17, 16]. We see in figure 11 that, for the chosen parameters in this plot, the predicted rates are above the present experimental bound for $M_{\rm SUSY} < 300\,\text{GeV}$.

Similarly to the $\tau \to 3\mu$ channel, the semileptonic $\tau \to \mu PP$ decays (with the exception of $\tau \to \mu\pi^0\pi^0$) are clearly dominated by the photon contribution and therefore they can be better approximated by the corresponding simplified formulas of this contribution. By neglecting the μ mass we have found the following approximate result,

$$\begin{aligned}\text{BR}(\tau \to \mu PP)_{\gamma_{\rm approx}} = &\int_{4m_P^2}^{m_\tau^2} ds \left(1 - \frac{s}{m_\tau^2}\right)^2 \left(1 + \frac{2m_\tau^2}{s}\right)\left(1 - \frac{4m_P^2}{s}\right)^{3/2} |F_V^{PP}(s)|^2 \\ &\times \frac{\alpha}{24\,m_\tau^2}\text{BR}(\tau \to \mu\gamma). \end{aligned} \tag{4.14}$$

JHEP06(2008)079

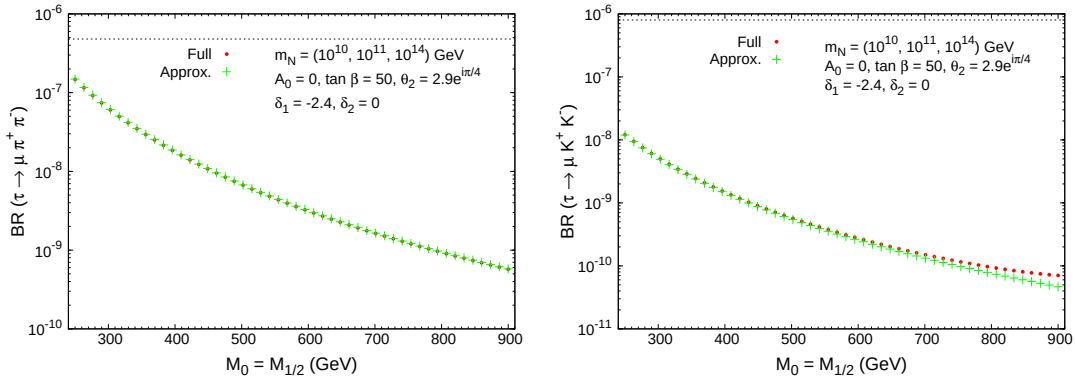

Figure 12: Comparison between the full rates and the approximate results in the NUHM scenario by considering just the photon-mediated contributions for $\tau \to \mu\pi^+\pi^-$ (left panel) and $\tau \to \mu K^+ K^-$ (right panel) as a function of $M_{\rm SUSY} = M_0 = M_{1/2}$. The dashed horizontal lines are the present experimental upper bounds [25].

And from this we get,

$$\begin{aligned}
\mathrm{BR}(\tau \to \mu\pi^+\pi^-)_{\gamma_{\rm approx}} &= 2.5 \times 10^{-3}\ \mathrm{BR}(\tau \to \mu\gamma) \\
&= 3.7 \times 10^{-5}\, |\delta_{32}|^2 \left(\frac{100}{M_{\rm SUSY}(\mathrm{GeV})}\right)^4 \left(\frac{\tan\beta}{60}\right)^2 , \quad (4.15) \\
\mathrm{BR}(\tau \to \mu K^+ K^-)_{\gamma_{\rm approx}} &= 2.0 \times 10^{-4}\ \mathrm{BR}(\tau \to \mu\gamma) \\
&= 3.0 \times 10^{-6}\, |\delta_{32}|^2 \left(\frac{100}{M_{\rm SUSY}(\mathrm{GeV})}\right)^4 \left(\frac{\tan\beta}{60}\right)^2 , \quad (4.16) \\
\mathrm{BR}(\tau \to \mu K^0 \bar{K}^0)_{\gamma_{\rm approx}} &= 1.2 \times 10^{-4}\ \mathrm{BR}(\tau \to \mu\gamma) \\
&= 1.8 \times 10^{-6}\, |\delta_{32}|^2 \left(\frac{100}{M_{\rm SUSY}(\mathrm{GeV})}\right)^4 \left(\frac{\tan\beta}{60}\right)^2 , \quad (4.17) \\
\mathrm{BR}(\tau \to \mu\rho)_{\gamma_{\rm approx}} &= 2.3 \times 10^{-3}\ \mathrm{BR}(\tau \to \mu\gamma) \\
&= 3.4 \times 10^{-5}\, |\delta_{32}|^2 \left(\frac{100}{M_{\rm SUSY}(\mathrm{GeV})}\right)^4 \left(\frac{\tan\beta}{60}\right)^2 , \quad (4.18) \\
\mathrm{BR}(\tau \to \mu\phi)_{\gamma_{\rm approx}} &= 8.4 \times 10^{-5}\ \mathrm{BR}(\tau \to \mu\gamma) \\
&= 1.3 \times 10^{-6}\, |\delta_{32}|^2 \left(\frac{100}{M_{\rm SUSY}(\mathrm{GeV})}\right)^4 \left(\frac{\tan\beta}{60}\right)^2 . \quad (4.19)
\end{aligned}$$

As can be clearly seen in figure 12 these results approach pretty well the full rates for most of the $M_{\rm SUSY}$ studied region. For $\mathrm{BR}(\tau \to \mu\pi^+\pi^-)$, they are indeed indistinguishable in this plot. It is only at very large $M_{\rm SUSY} \geq 750$ GeV that the approximate result of $\mathrm{BR}(\tau \to \mu K^+ K^-)$ separates slightly from the full result, due to the Higgs contribution which competes with the photon one in this region.

For completeness and comparison, we also include here the predictions for the leading LFV tau decay channel, $\tau \to \mu\gamma$. Figure 13 displays the predictions of the full and approximate rates for this $\tau \to \mu\gamma$ channel. The full rates are taken from [21] and the

JHEP06(2008)079

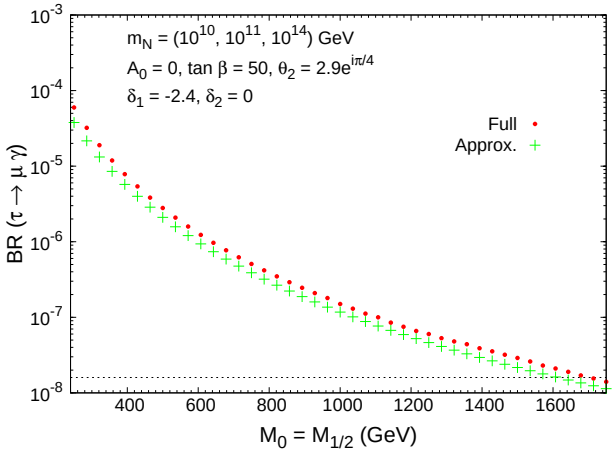

Figure 13: Comparison between the full 1-loop prediction [2] and approximate results of eq. (4.20) for $\tau \to \mu\gamma$ as a function of $M_{\rm SUSY} = M_0 = M_{1/2}$ in the NUHM scenario. The horizontal line is the present experimental upper bound [15].

approximate ones are given by the result of the MI approach [33, 3], which at large $\tan\beta$ and for equal SUSY mass scales is,

$$\begin{aligned} \mathrm{BR}(\tau \to \mu\gamma)_{\rm approx} &= \frac{\alpha^3}{14400\pi^2}\frac{m_\tau^5}{\Gamma_\tau \sin^4\theta_W}\frac{|\delta_{32}|^2}{M_{\rm SUSY}^4}(\tan\beta)^2 \\ &= 1.5\times 10^{-2}\,|\delta_{32}|^2\left(\frac{100}{M_{\rm SUSY}(\mathrm{GeV})}\right)^4\left(\frac{\tan\beta}{60}\right)^2 . \end{aligned} \tag{4.20}$$

In this case, and for the chosen parameters in this plot, the approximate and the full results agree to better than a factor 2. We have verified, however, that for other choices of $\delta_{1,2}$ the difference between them can be larger. Regarding this difference, we emphasise that in using the MI approach and LLog approximation one has to be carefull because they are known to fail in some regions of the CMSSM parameter space. For instance, in [53], the departure of the MI from the exact result is estimated to be up to 50% for $|\delta_{32}| \sim 1$. In [22] it has been found that the use of the MI and LLog for large trilinear couplings, $A_0 \sim \mathcal{O}$ (1 TeV), can fail in several orders of magnitude.

The most evident conclusion from figure 13 is that for the chosen parameters in this plot and for $M_{\rm SUSY} < 1600$ GeV, the $\tau \to \mu\gamma$ rates are above the present experimental sensitivity, therefore this tau decay channel is at present the most competitive one in setting bounds on the tau-muon LFV. However, besides experimental issues, the limitation of this channel is that it is not sensitive at all to the Higgs sector. In this sense, the semileptonic channels are more interesting, and can be clearly competitive in the large $M_{\rm SUSY} \sim \mathcal{O}(1 - 2\,\mathrm{TeV})$ region.

In figures 14 and 15 we plot finally the predictions for $\mathrm{BR}(\tau \to \mu K^+K^-)$ and $\mathrm{BR}(\tau \to \mu\eta)$ as a function of one the most relevant parameters for these Higgs-mediated processes which is the corresponding Higgs boson mass.

JHEP06(2008)079

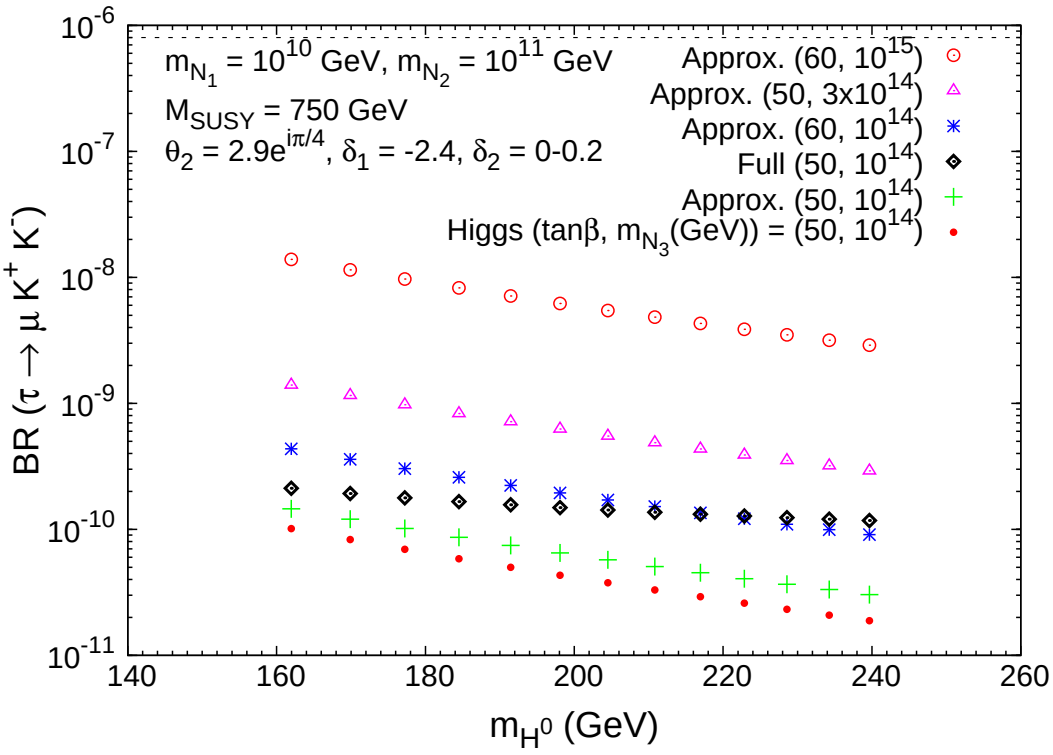

Figure 14: Predictions for BR($\tau \to \mu K^+ K^-$) as a function of m_{H^0} in the NUHM scenario. A comparison between the full 1-loop computation and the approximation given by eq. (4.5) for various choices of large $\tan\beta$ and m_{N_3} is included. The horizontal line is the present experimental upper bound [25].

Firstly, we see again that the approximate and exact results of the Higgs contribution agree within a factor of two for both channels, but the agreement of the full result with respect to the Higgs contribution is clearly worse in the case of $\tau \to \mu K^+ K^-$ than in $\tau \to \mu\eta$. In the latter, the agreement is quite good because the Z-mediated contribution is negligible, and this holds for all $M_{\rm SUSY}$ values in the studied interval, 250 GeV $< M_{\rm SUSY} <$ 750 GeV . In the first, it is only for large $M_{\rm SUSY}$ that the H-mediated contribution competes with the γ-mediated one and the Higgs rates approach the total rates. For instance, figure 14 shows that for $M_{\rm SUSY} = 750$ GeV and $m_{H^0} = 160$ GeV the total rate is about a factor 2 above the Higgs rate, but for $m_{H^0} = 240$ GeV it is already more than a factor 5 above.

In these figures we have also explored larger values of m_{N_3} and $\tan\beta$, by using in those cases the approximate formula, and in order to conclude about the values that predict rates comparable with the present experimental sensitivity. We can conclude then that, at present, it is certainly $\tau \to \mu\eta$ the most competitive LFV semileptonic tau decay channel. The parameter values that provide rates being comparable to the present sensitivities in this channel are $\tan\beta = 60$ and $m_{N_3} = 10^{15}$ GeV which correspond to $|\delta_{32}| \simeq 2$. These large rates, however, should be taken with care and be considered just as an order of magnitude

JHEP06(2008)079

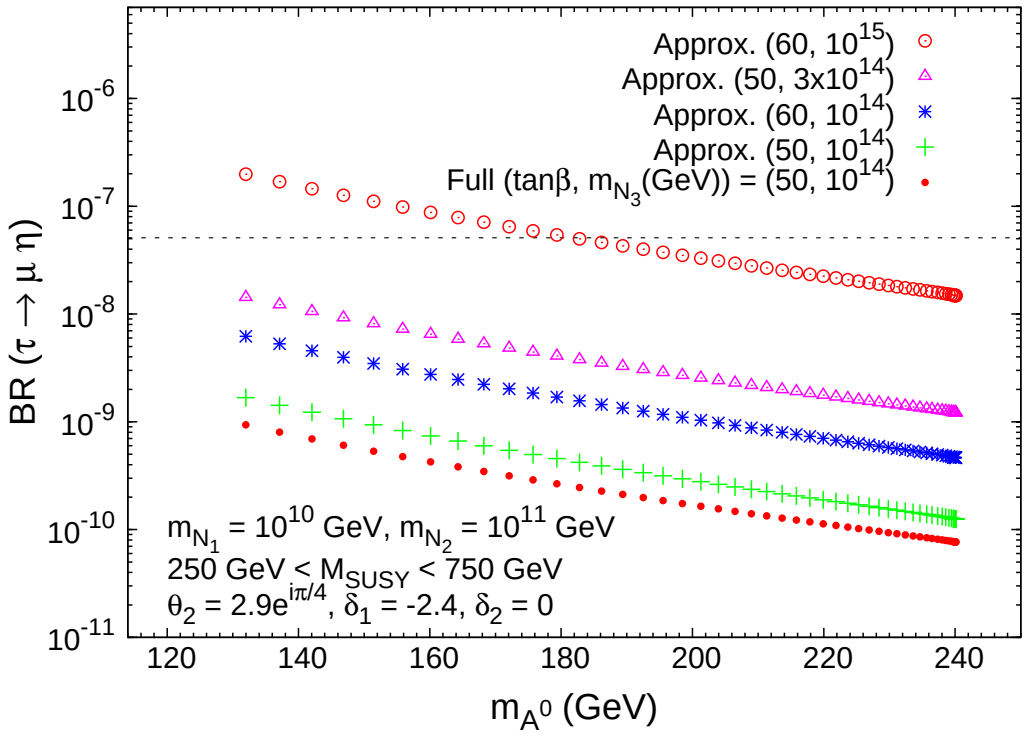

Figure 15: Predictions for BR($\tau \to \mu\eta$) as a function of m_{A^0} in the NUHM scenario. A comparison between the full 1-loop computation and the approximation given by eq. (4.5) for various choices of large $\tan\beta$ and m_{N_3} is included. The horizontal line is the present experimental upper bound [15].

estimate since, as we have explained in section 2.1, they correspond to neutrino Yukawa couplings which are clearly in the non-perturbative regime. This is why we do not provide the corresponding full rates for them.

5. Conclusions

In this paper we have presented a complete one-loop computation of the branching ratios for the LFV semileptonic τ decays within the context of two constrained MSSM-seesaw scenarios, the CMSSM and the NUHM. We have included both analytical and numerical results for the particular channels: $\tau \to \mu PP$, with $PP = \pi^+\pi^-, \pi^0\pi^0, K^+K^-, K^0\bar{K}^0$; $\tau \to \mu P$ with $P = \pi, \eta, \eta'$; and $\tau \to \mu\rho$, $\tau \to \mu\phi$. The analysis of the channels $\tau \to \mu PP$, with $PP = \pi^+\pi^-, \pi^0\pi^0, K^0\bar{K}^0$, and $\tau \to \mu\rho$, $\tau \to \mu\phi$ are, to our knowledge, the first ones in the literature within the CMSSM-seesaw context. In addition, we have compared our predictions for $\tau \to \mu K^+K^-$ and for $\tau \to \mu P$ with $P = \pi, \eta, \eta'$ with previous predictions in the literature and found some discrepancies.

Our treatment of hadronisation has involved two different procedures : for the γ contribution we have employed state of the art form factors (detailed in appendix B), as this amplitude is fairly dominated by resonance states; for heavier intermediate contributions

JHEP06(2008)079

(Z and Higgses) we have a local (point-like) vertex driven by chiral symmetry. It is difficult to estimate the errors of this procedure. For the hadronization of the γ, large-N_C inspired, the error should be smaller than 30% [46] (at amplitude level), based on the fact that subleading terms in the expansion have been included through the widths of resonances. The hadronization of currents driven by the Z or Higgses, on the other side, is less known and it is not possible to give a reliable error estimate.

Our results for $\tau \to \mu\pi^+\pi^-$ demonstrate that this channel is clearly dominated by the photon-mediated contribution in all the studied region of $100\,\text{GeV} < M_{\text{SUSY}} < 1000\,\text{GeV}$. In fact it is by far, the $\tau \to \mu PP$ channel with the highest rates, reaching values close to its present experimental bound at 4.8×10^{-7} for some input parameter values. Concretely, it happens for low $M_{\text{SUSY}} \sim 100{-}200\,\text{GeV}$, large $\tan\beta \sim 50{-}60$, large $m_{N_3} \sim 10^{14}{-}10^{15}\,\text{GeV}$ and large $\arg(\theta_2) \sim \pi/4 - \pi/2$ (these two latter parameters producing a large $\delta_{32} \sim \mathcal{O}(1)$). In contrast, $\tau \to \mu\pi^0\pi^0$ can only be mediated by h^0 and H^0 Higgs bosons and their rates are very small. Besides, they are not yet comparable with data, since there is no bound in this channel. The cases of $\tau \to \mu K^+K^-$ and $\tau \to \mu K^0\bar{K}^0$ decays, are much more interesting. In these two channels, the photon-mediated contribution dominates in most of the studied region of M_{SUSY}, except at large, $M_{\text{SUSY}} > 750\,\text{GeV}$ values, where the Higgs-mediated and the γ-mediated contributions can compete. This competition happens in specific constrained scenarios of NUHM type with low $m_{H^0} \sim 100 - 200\,\text{GeV}$ values and very heavy SUSY spectrum with $M_{\text{SUSY}} > 750\,\text{GeV}$. This peculiar MSSM spectrum and the fact that Higgs bosons couple stronger to K^+K^- (and $K^0\bar{K}^0$) than to $\pi^+\pi^-$ (and $\pi^0\pi^0$) is the reason why the H- and γ-mediated contributions can compete in $\tau \to \mu K^+K^-$ but not in $\tau \to \mu\pi^+\pi^-$. Furthermore, due to the fact that the photon diagram still dominates $\text{BR}(\tau \to \mu K^+K^-)$ in a large region of the parameter space with $100\,\text{GeV} < M_{\text{SUSY}} < 750\,\text{GeV}$, the involved hadronic form factors do play a crutial role in the final rates. Consequently, our results for this channel are in disagreement with those of [34] where they only included the Higgs-mediated contribution. We have also shown that the largest predicted rates for $\text{BR}(\tau \to \mu K^+K^-)$ are, as in $\tau \to \mu\pi^+\pi^-$, at the region with low $M_{\text{SUSY}} \sim 100 - 200\,\text{GeV}$, large $\tan\beta \sim 50 - 60$, large $m_{N_3} \sim 10^{14} - 10^{15}\,\text{GeV}$ and large $\arg(\theta_2) \sim \pi/4 - \pi/2$ values. However, the predicted rates do not reach yet the present experimental sensitivity, which in this channel is at 8×10^{-7}.

Our results for $\tau \to \mu\eta$ and $\tau \to \mu\eta'$ demonstrate that these two channels are largely dominated by the A^0-mediated contribution and their predicted rates are very competitive in the case of NUHM scenarios with low $m_{A^0} \sim 100 - 200\,\text{GeV}$ values and large $\tan\beta \sim 50{-}60$. This is in qualitative agreement with previous estimates in the literature. However, we have found some important numerical discrepancies with respect to the estimate in [31]. Concretely, the predicted rates in the present work are smaller than those in [31] by a factor of about 7. We believe that these discrepancies are due to the different procedures of quark bilinear hadronisation. We claim that our results which are based on the well defined and more refined hadronisation prescription by χPT provide a better estimate. The rates for $\text{BR}(\tau \to \mu\eta)$ have also been compared with those in [32, 33] which are within the different context of non-constrained MSSM and with input δ_{32} not being connected to neutrino physics nor seesaw mechanism. We have checked, that the predicted rates are in

reasonable agreement with these two works for, $\delta_{32} \sim \mathcal{O}(1)$, which in our case is reached by input seesaw parameters of $m_{N_3} \sim 10^{14} - 10^{15}$ GeV and large $\arg(\theta_2) \sim \pi/4 - \pi/2$.

In addition, we have presented in this work a set of useful approximate formulas for all the semileptonic τ decays that we have compared with the full-one loop results and concluded that they give reasonable good estimates, say differing in less than a factor of two respect to the full result. We have also compared these results with those for the leptonic channel, $\tau \to 3\mu$, and the radiative decay, $\tau \to \mu\gamma$.

Our overall conclusion is that, for the same Constrained MSSM-Seesaw input parameters, $\tau \to \mu\gamma$ is the most competitive τ decay channel in testing the values of the LFV parameter δ_{32}, but it is not sensitive at all to the Higgs sector. Interestingly, the most competitive channels to explore simultaneously LFV and the Higgs sector are $\tau \to \mu\eta$, $\tau \to \mu\eta'$ and also $\tau \to \mu K^+K^-$. The $\tau \to \mu K^+K^-$ channel is certainly more efficient than $\tau \to 3\,\mu$ as far as the sensitivity to the Higgs sector is concerned. Otherwise, the golden channels to tackle the Higgs sector are undoubtly $\tau \to \mu\eta$ and $\tau \to \mu\eta'$. On the other hand, the rest of the studied semileptonic channels, $\tau \to \mu\pi^+\pi^-$, etc., will not provide additional information on LFV with respect to that provided by $\tau \to \mu\gamma$.

Acknowledgments

We acknowledge P. Paradisi for clarifying us the results of the $\tau \to \mu\gamma$ in the mass insertion approximation. This work has been supported in part by the EU MRTN-CT-2006-035482 (FLAVIAnet), by MEC (Spain) under grants FPA2006-05423 and FPA2007-60323, by Generalitat Valenciana under grant GVACOMP2007-156, by Comunidad de Madrid under HEPHACOS project and by the Spanish Consolider-Ingenio 2010 Programme CPAN (CSD2007-00042).

A. LFV form factors

In this appendix we collect the main analytical formulae containing the full 1-loop results of the SUSY contributions to the relevant $\tau - \mu$ LFV form factors for the present work, corresponding to: $\gamma\tau\mu$, $Z\tau\mu$ and $H\tau\mu$ vertices. All the couplings and loop functions appearing in the following formulae are defined in [21, 24].

A.1 Form factors for the $\gamma\tau\mu$ vertex

Our convention for the form factors $A_{1,2}^{L,R}$ defining the $\gamma\tau\mu$ vertex is as follows:

$$ie\left[q^2\gamma_\alpha(A_1^L P_L + A_1^R P_R) + im_\tau\sigma_{\alpha\beta}q^\beta(A_a^L P_L + A_2^R P_R)\right], \tag{A.1}$$

where q is the off-shell photon momentum, $P_{L,R} = (1 \mp \gamma_5)/2$, e is the electromagnetic positron charge and m_τ is the τ lepton mass.

In the SUSY-seesaw context there are one-loop contributions to these form factors that come from the chargino and neutralino sectors respectively,

$$A_a^{L,R} = A_a^{(n)L.R} + A_a^{(c)L,R}, \quad a = 1, 2\,. \tag{A.2}$$

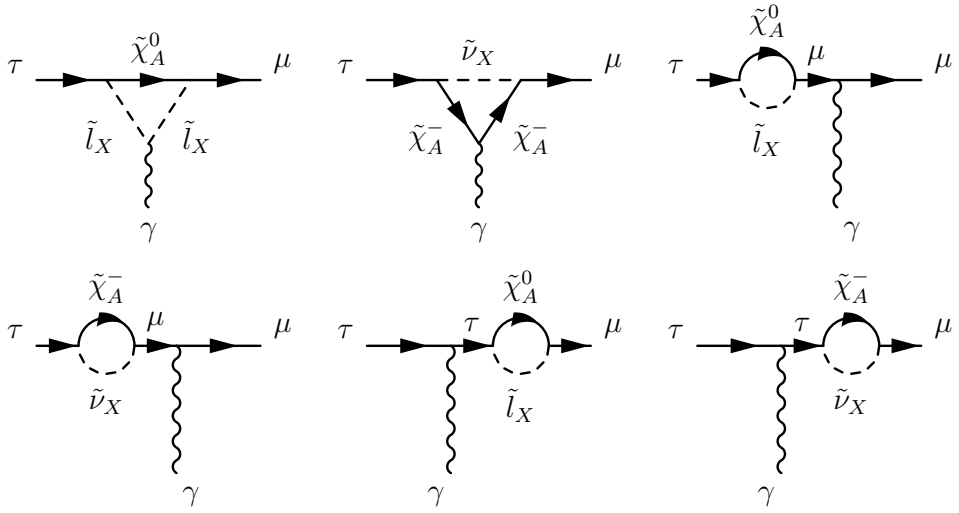

Figure 16: Relevant SUSY one-loop diagrams for the photon-mediated contributions to LFV semileptonic τ decays.

The neutralino contributions are given by,

$$A_1^{(n)L} = \frac{1}{576\pi^2} N^R_{\mu AX} N^{R*}_{\tau AX} \frac{1}{m^2_{\tilde{l}_X}} \frac{2 - 9x_{AX} + 18x_{AX}^2 - 11x_{AX}^3 + 6x_{AX}^3 \log x_{AX}}{(1-x_{AX})^4}$$

$$\begin{aligned} A_2^{(n)L} = \frac{1}{32\pi^2} \frac{1}{m^2_{\tilde{l}_X}} \Bigg[& N^L_{\mu AX} N^{L*}_{\tau AX} \frac{1 - 6x_{AX} + 3x_{AX}^2 + 2x_{AX}^3 - 6x_{AX}^2 \log x_{AX}}{6\,(1-x_{AX})^4} \\ & + N^R_{\mu AX} N^{R*}_{\tau AX} \frac{m_\mu}{m_\tau} \frac{1 - 6x_{AX} + 3x_{AX}^2 + 2x_{AX}^3 - 6x_{AX}^2 \log x_{AX}}{6\,(1-x_{AX})^4} \\ & + N^L_{\mu AX} N^{R*}_{\tau AX} \frac{m_{\tilde{\chi}_A^0}}{m_\tau} \frac{1 - x_{AX}^2 + 2x_{AX} \log x_{AX}}{(1-x_{AX})^3} \Bigg], \end{aligned} \tag{A.3}$$

$$A_a^{(n)R} = A_a^{(n)L}\Big|_{L \leftrightarrow R}, \tag{A.4}$$

where $x_{AX} = m^2_{\tilde{\chi}_A^0}/m^2_{\tilde{l}_X}$ and the indices are $A = 1, \ldots, 4$, $X = 1, \ldots, 6$.

The chargino contributions are given by

$$A_1^{(c)L} = -\frac{1}{576\pi^2} C^R_{\mu AX} C^{R*}_{\tau AX} \frac{1}{m^2_{\tilde{\nu}_X}} \frac{16 - 45x_{AX} + 36x_{AX}^2 - 7x_{AX}^3 + 6(2 - 3x_{AX}) \log x_{AX}}{(1-x_{AX})^4},$$

$$\begin{aligned} A_2^{(c)L} = -\frac{1}{32\pi^2} \frac{1}{m^2_{\tilde{\nu}_X}} \Bigg[& C^L_{\mu AX} C^{L*}_{\tau AX} \frac{2 + 3x_{AX} - 6x_{AX}^2 + x_{AX}^3 + 6x_{AX} \log x_{AX}}{6\,(1-x_{AX})^4} \\ & + C^R_{\mu AX} C^{R*}_{\tau AX} \frac{m_\mu}{m_\tau} \frac{2 + 3x_{AX} - 6x_{AX}^2 + x_{AX}^3 + 6x_{AX} \log x_{AX}}{6\,(1-x_{AX})^4} \\ & + C^L_{\mu AX} C^{R*}_{\tau AX} \frac{m_{\tilde{\chi}_A^-}}{m_\tau} \frac{-3 + 4x_{AX} - x_{AX}^2 - 2\log x_{AX}}{(1-x_{AX})^3} \Bigg], \end{aligned} \tag{A.5}$$

$$A_a^{(c)R} = A_a^{(c)L}\Big|_{L \leftrightarrow R}, \tag{A.6}$$

JHEP06(2008)079

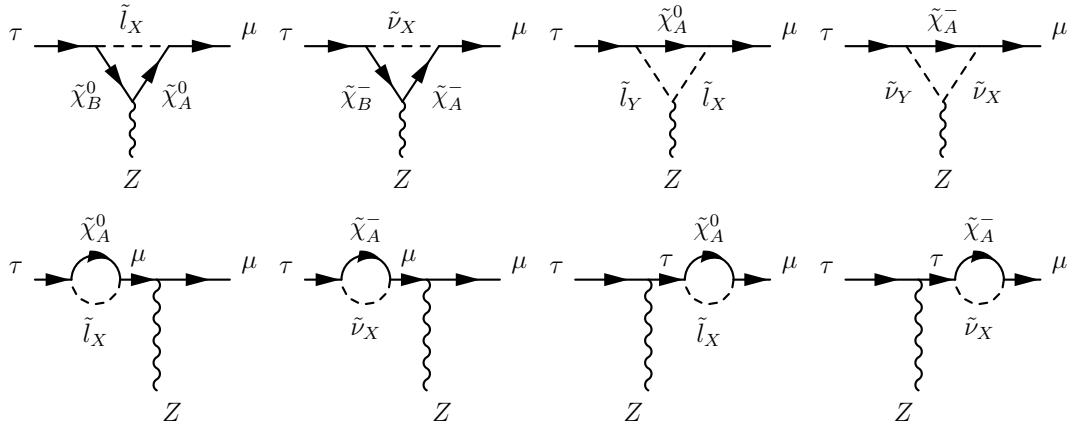

Figure 17: Relevant SUSY one-loop diagrams for the Z-mediated contributions to LFV semileptonic τ decays.

where in this case $x_{AX} = m^2_{\tilde{\chi}^-_A}/m^2_{\tilde{\nu}_X}$ and the indices are $A = 1, 2$, $X = 1, 2, 3$. Notice that in both neutralino and chargino contributions a summation over the indices A and X is understood.

A.2 Form factors for the $Z\tau\mu$ vertex

Our convention for the form factors $F_{L,R}$ defining the $Z\tau\mu$ vertex is as follows:

$$-i\gamma_\mu \left[F_L P_L + F_R P_R\right]. \tag{A.7}$$

The Z-boson form factors have also the two kinds of contributions, from neutralinos (n) and charginos (c),

$$F_{L(R)} = F^{(n)}_{L(R)} + F^{(c)}_{L(R)}\,. \tag{A.8}$$

The results for the corresponding form factors are the following:

$$\begin{aligned}
F^{(n)}_L = -\frac{1}{16\pi^2}\Big\{ & N^R_{\mu BX} N^{R*}_{\tau AX}\Big[2E^{R(n)}_{BA} C_{24}(m^2_{\tilde{l}_X}, m^2_{\tilde{\chi}^0_A}, m^2_{\tilde{\chi}^0_B}) \\
& - E^{L(n)}_{BA} m_{\tilde{\chi}^0_A} m_{\tilde{\chi}^0_B} C_0(m^2_{\tilde{l}_X}, m^2_{\tilde{\chi}^0_A}, m^2_{\tilde{\chi}^0_B})\Big] \\
& + N^R_{\mu AX} N^{R*}_{\tau AY}\Big[2Q^{\tilde{l}}_{XY} C_{24}(m^2_{\tilde{\chi}^0_A}, m^2_{\tilde{l}_X}, m^2_{\tilde{l}_Y})\Big] \\
& + N^R_{\mu AX} N^{R*}_{\tau AX}\Big[Z^{(l)}_L B_1(m^2_{\tilde{\chi}^0_A}, m^2_{\tilde{l}_X})\Big]\Big\}, \\
F^{(n)}_R = & \left. F^{(n)}_L\right|_{L\leftrightarrow R}, \\
F^{(c)}_L = -\frac{1}{16\pi^2}\Big\{ & C^R_{\mu BX} C^{R*}_{\tau AX}\Big[2E^{R(c)}_{BA} C_{24}(m^2_{\tilde{\nu}_X}, m^2_{\tilde{\chi}^-_A}, m^2_{\tilde{\chi}^-_B}) \\
& - E^{L(c)}_{BA} m_{\tilde{\chi}^-_A} m_{\tilde{\chi}^-_B} C_0(m^2_{\tilde{\nu}_X}, m^2_{\tilde{\chi}^-_A}, m^2_{\tilde{\chi}^-_B})\Big]
\end{aligned}$$

JHEP06(2008)079

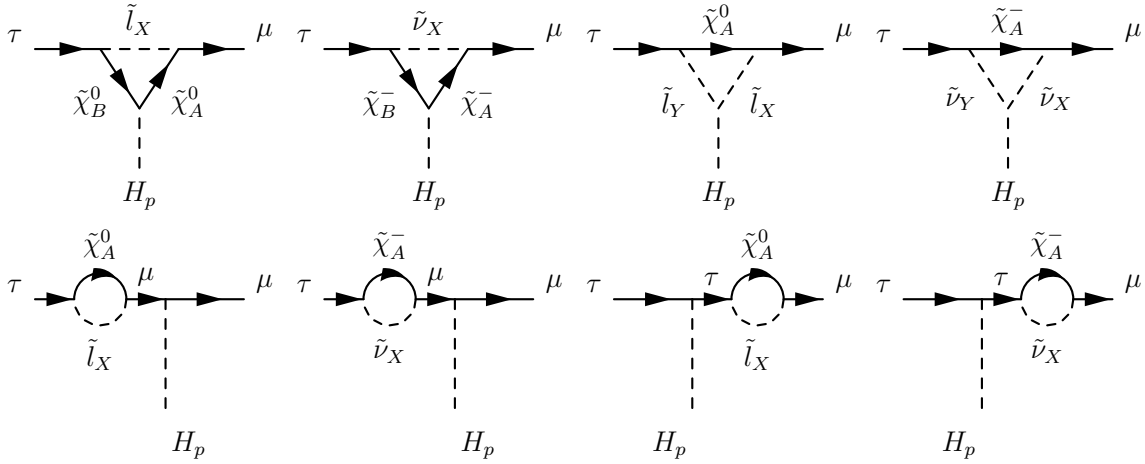

Figure 18: Relevant SUSY one-loop diagrams for the Higgs-mediated contributions to LFV semileptonic τ decays.

$$+C^R_{\mu AX}C^{R*}_{\tau AY}\Big[2Q^{\tilde{\nu}}_{XY}C_{24}(m^2_{\tilde{\chi}^-_A},m^2_{\tilde{\nu}_X},m^2_{\tilde{\nu}_Y})\Big]$$
$$+C^R_{\mu AX}C^{R*}_{\tau AX}\Big[Z^{(l)}_L B_1(m^2_{\tilde{\chi}^-_A},m^2_{\tilde{\nu}_X})\Big]\Big\},$$
$$F^{(c)}_R = F^{(c)}_L\Big|_{L\leftrightarrow R}, \tag{A.9}$$

where again the indices are $A,B=1,\ldots,4$, $X,Y=1,\ldots,6$ in the contributions from the neutralino sector and $A,B=1,2$, $X,Y=1,2,3$ in the contributions from the chargino sector, and a summation over the various indices is understood.

A.3 Form factors for the $H\tau\mu$ vertex

Our convention for the form factors $H^{(p)}_{L,R}$ defining the $H_p\tau\mu$ vertex is as follows:

$$i\left[H^{(p)}_L P_L + H^{(p)}_R P_R\right]. \tag{A.10}$$

As in the previous cases, we separate the contributions from the neutralino and chargino sectors,

$$H^{(p)}_{L(R)} = H^{(p)}_{L(R),n} + H^{(p)}_{L(R),c}. \tag{A.11}$$

The results for the form factors are the following,

$$H^{(p)}_{L,n} = -\frac{1}{16\pi^2}\Big\{\Big[B_0(m^2_{\tilde{\chi}^0_A},m^2_{\tilde{\chi}^0_B}) + m^2_{\tilde{l}_X}C_0(m^2_{\tilde{l}_X},m^2_{\tilde{\chi}^0_A},m^2_{\tilde{\chi}^0_B}) + m^2_\tau C_{12}(m^2_{\tilde{l}_X},m^2_{\tilde{\chi}^0_A},m^2_{\tilde{\chi}^0_B})$$
$$+ m^2_\mu(C_{11}-C_{12})(m^2_{\tilde{l}_X},m^2_{\tilde{\chi}^0_A},m^2_{\tilde{\chi}^0_B})\Big]N^L_{\mu AX}D^{(p)}_{R,AB}N^{R*}_{\tau BX}$$
$$+m_\mu m_\tau(C_{11}+C_0)(m^2_{\tilde{l}_X},m^2_{\tilde{\chi}^0_A},m^2_{\tilde{\chi}^0_B})N^R_{\mu AX}D^{(p)}_{L,AB}N^{L*}_{\tau BX}$$
$$+m_\mu m_{\tilde{\chi}^0_B}(C_{11}-C_{12}+C_0)(m^2_{\tilde{l}_X},m^2_{\tilde{\chi}^0_A},m^2_{\tilde{\chi}^0_B})N^R_{\mu AX}D^{(p)}_{L,AB}N^{R*}_{\tau BX}$$

$$
\begin{aligned}
&+m_\tau m_{\tilde{\chi}^0_B} C_{12}(m^2_{\tilde{l}_X}, m^2_{\tilde{\chi}^0_A}, m^2_{\tilde{\chi}^0_B}) N^L_{\mu AX} D^{(p)}_{R,AB} N^{L*}_{\tau BX} \\
&+m_\mu m_{\tilde{\chi}^0_A} (C_{11} - C_{12})(m^2_{\tilde{l}_X}, m^2_{\tilde{\chi}^0_A}, m^2_{\tilde{\chi}^0_B}) N^R_{\mu AX} D^{(p)}_{R,AB} N^{R*}_{\tau BX} \\
&+m_\tau m_{\tilde{\chi}^0_A} (C_{12} + C_0)(m^2_{\tilde{l}_X}, m^2_{\tilde{\chi}^0_A}, m^2_{\tilde{\chi}^0_B}) N^L_{\mu AX} D^{(p)}_{L,AB} N^{L*}_{\tau BX} \\
&+m_{\tilde{\chi}^0_A} m_{\tilde{\chi}^0_B} C_0(m^2_{\tilde{l}_X}, m^2_{\tilde{\chi}^0_A}, m^2_{\tilde{\chi}^0_B}) N^L_{\mu AX} D^{(p)}_{L,AB} N^{R*}_{\tau BX} \\
&+G^{(p)\tilde{l}}_{XY} \Big[-m_\mu (C_{11} - C_{12})(m^2_{\tilde{\chi}^0_A}, m^2_{\tilde{l}_X}, m^2_{\tilde{l}_Y}) N^R_{\mu AX} N^{R*}_{\tau AY} \\
&- m_\tau C_{12}(m^2_{\tilde{\chi}^0_A}, m^2_{\tilde{l}_X}, m^2_{\tilde{l}_Y}) N^L_{\mu AX} N^{L*}_{\tau AY} + m_{\tilde{\chi}^0_A} C_0(m^2_{\tilde{\chi}^0_A}, m^2_{\tilde{l}_X}, m^2_{\tilde{l}_Y}) N^L_{\mu AX} N^{R*}_{\tau AY} \Big] \\
&+\frac{S^{(p)}_{L,\tau}}{m^2_\mu - m^2_\tau} \Big[-m^2_\mu B_1(m^2_{\tilde{\chi}^0_A}, m^2_{\tilde{l}_X}) N^L_{\mu AX} N^{L*}_{\tau AX} + m_\mu m_{\tilde{\chi}^0_A} B_0(m^2_{\tilde{\chi}^0_A}, m^2_{\tilde{l}_X}) N^R_{\mu AX} N^{L*}_{\tau AX} \\
&- m_\mu m_\tau B_1(m^2_{\tilde{\chi}^0_A}, m^2_{\tilde{l}_X}) N^R_{\mu AX} N^{R*}_{\tau AX} + m_\tau m_{\tilde{\chi}^0_A} B_0(m^2_{\tilde{\chi}^0_A}, m^2_{\tilde{l}_X}) N^L_{\mu AX} N^{R*}_{\tau AX} \Big] \\
&+\frac{S^{(p)}_{L,\mu}}{m^2_\tau - m^2_\mu} \Big[-m^2_\tau B_1(m^2_{\tilde{\chi}^0_A}, m^2_{\tilde{l}_X}) N^R_{\mu AX} N^{R*}_{\tau AX} + m_\tau m_{\tilde{\chi}^0_A} B_0(m^2_{\tilde{\chi}^0_A}, m^2_{\tilde{l}_X}) N^R_{\mu AX} N^{L*}_{\tau AX} \\
&- m_\mu m_\tau B_1(m^2_{\tilde{\chi}^0_A}, m^2_{\tilde{l}_X}) N^L_{\mu AX} N^{L*}_{\tau AX} + m_\mu m_{\tilde{\chi}^0_A} B_0(m^2_{\tilde{\chi}^0_A}, m^2_{\tilde{l}_X}) N^L_{\mu AX} N^{R*}_{\tau AX} \Big] \Big\}, \qquad \text{(A.12)}
\end{aligned}
$$

$$
H^{(p)}_{R,n} = H^{(p)}_{L,n}\Big|_{L \leftrightarrow R} \quad p = 1, 2, 3. \qquad \text{(A.13)}
$$

Correspondingly, the result for the chargino contribution $H^{(p)}_{L(R),c}$ can be obtained from the previous $H^{(p)}_{L(R),n}$ by replacing everywhere,

$$
\begin{aligned}
\tilde{l} &\to \tilde{\nu} \\
\tilde{\chi}^0 &\to \tilde{\chi}^- \\
N^{L(R)} &\to C^{L(R)} \\
D_{L(R)} &\to W_{L(R)}
\end{aligned}
$$

In the previous formulae, the index p refers to the each of the Higgs bosons. Concretely, $H_p = h^0, H^0, A^0$ for $p = 1, 2, 3$, respectively. The other indices are again $A, B = 1, \ldots, 4$, $X, Y = 1, \ldots, 6$ in the contributions from the neutralino sector and $A, B = 1, 2$ and $X, Y = 1, 2, 3$ in the contributions from the chargino sector. A summation over all the indices is also understood.

B. Hadronic form factors

Our construction of the vector form factors $F_V^{PP}(s)$, defined by eq. (2.28), follows the idea put forward in [54] that lie on two key points :

1/ At $s \ll M_R^2$ (being M_R a generic resonance mass), the vector form factor should match the $\mathcal{O}(p^4)$ result of χPT. Hence our form factors will satisfy the chiral constraint.

2/ Form factors of QCD currents should behave softly at high transfer of momenta [38], i.e. they should vanish for $s \gg M_R^2$. Accordingly we will demand to our form factors that they satisfy this asymptotic constraint.

In the $N_C \to \infty$ limit resonances have zero-width. However those present in the relevant form factors in tau decays do indeed resonate due to the available phase space. As a consequence we need to include energy-dependent widths for the wider resonances $\rho(770)$ and $\rho(1450)$, or constant for the narrow ones : $\omega(782)$ and $\phi(1020)$. For the $\rho(770)$ we take the definition put forward in [55] :

$$\Gamma_\rho(s) = \frac{M_\rho s}{96\pi F^2}\left[\sigma_\pi^3(s)\,\theta(\,s\,-\,4m_\pi^2) \,+\, \frac{1}{2}\,\sigma_K^3(s)\,\theta(\,s\,-\,4m_K^2)\right] , \tag{B.1}$$

where $\sigma_P(s) = \sqrt{1-4\frac{m_P^2}{s}}$, while for $\rho(1450)$ we employ a reasonable parameterisation :

$$\Gamma_{\rho'}(s) = \Gamma_{\rho'}(M_{\rho'}^2)\,\frac{s}{M_{\rho'}^2}\,\left(\frac{\sigma_\pi^3(s)\;+\,\frac{1}{2}\,\sigma_K^3(s)\,\theta(\,s\,-\,4m_K^2)}{\sigma_\pi^3(M_{\rho'}^2)\,+\,\frac{1}{2}\,\sigma_K^3(M_{\rho'}^2)\,\theta(\,s\,-\,4m_K^2)}\right)\theta(\,s\,-\,4m_\pi^2)\,. \tag{B.2}$$

The $\mathcal{O}(p^4)$ determination of the vector form factors was done in [49]. Requiring that our expressions match that result at small transfer of momentum we get the following expressions :

$$\begin{aligned}
F_V^{\pi\pi}(s) &= F(s)\;\exp\left[2\,Re\left(\tilde{H}_{\pi\pi}(s)\right)\,+\,Re\left(\tilde{H}_{KK}(s)\right)\right] \qquad \text{(B.3)}\\
F(s) &= \frac{M_\rho^2}{M_\rho^2 - s - iM_\rho\Gamma_\rho(s)}\left[1+\left(\delta\,\frac{M_\omega^2}{M_\rho^2}\,-\,\gamma\,\frac{s}{M_\rho^2}\right)\,\frac{s}{M_\omega^2-s-iM_\omega\Gamma_\omega}\right]\\
&\quad -\frac{\gamma\,s}{M_{\rho'}^2 - s - iM_{\rho'}\Gamma_{\rho'}(s)}\;,\\
F_V^{K^+K^-}(s) &= \frac{1}{2}\,\frac{M_\rho^2}{M_\rho^2 - s - iM_\rho\Gamma_\rho(s)}\,\exp\left[2\,Re\left(\tilde{H}_{\pi\pi}(s)\right)\,+\,Re\left(\tilde{H}_{KK}(s)\right)\right]\\
&\quad +\frac{1}{2}\left[\sin^2\theta_V\,\frac{M_\omega^2}{M_\omega^2-s-iM_\omega\Gamma_\omega}\,+\,\cos^2\theta_V\,\frac{M_\phi^2}{M_\phi^2-s-iM_\phi\Gamma_\phi}\right]\\
&\quad \times\exp\left[3\,Re\left(\tilde{H}_{KK}(s)\right)\right]\,,\\
F_V^{K^0\bar{K}^0}(s) &= -\frac{1}{2}\,\frac{M_\rho^2}{M_\rho^2 - s - iM_\rho\Gamma_\rho(s)}\,\exp\left[2\,Re\left(\tilde{H}_{\pi\pi}(s)\right)\,+\,Re\left(\tilde{H}_{KK}(s)\right)\right]\\
&\quad +\frac{1}{2}\left[\sin^2\theta_V\,\frac{M_\omega^2}{M_\omega^2-s-iM_\omega\Gamma_\omega}\,+\,\cos^2\theta_V\,\frac{M_\phi^2}{M_\phi^2-s-iM_\phi\Gamma_\phi}\right]\\
&\quad \times\exp\left[3\,Re\left(\tilde{H}_{KK}(s)\right)\right]\,,
\end{aligned}$$

where we have used the definitions :

$$\begin{aligned}
\beta &= \frac{\Theta_{\rho\omega}}{3M_\rho^2}\,,\\
\gamma &= \frac{F_V G_V}{F^2}\,(1+\beta) - 1\,,\\
\delta &= \frac{F_V G_V}{F^2} - 1\,,\\
\tilde{H}_{PP}(s) &= \frac{s}{F^2}M_P(s)\,,
\end{aligned}$$

$$M_P(s) = \frac{1}{12}\left(1 - 4\frac{m_P^2}{s}\right) J_P(s) - \frac{k_P(M_\rho)}{6} + \frac{1}{288\pi^2} ,$$
$$J_P(s) = \frac{1}{16\pi^2}\left[\sigma_P(s) \ln\frac{\sigma_P(s)-1}{\sigma_P(s)+1} + 2\right] ,$$
$$k_P(\mu) = \frac{1}{32\pi^2}\left(\ln\frac{m_P^2}{\mu^2} + 1\right) . \tag{B.4}$$

Notice that the β parameter includes the contribution of the isospin breaking $\rho-\omega$ mixing through $\Theta_{\rho\omega} = -3.3\times10^{-3}\,\mathrm{GeV}^2$ [56], and F_V and G_V are defined in eq. (2.21). Moreover the asymptotic constraint on the $N_C \to \infty$ vector form factor indicates $F_V G_V \simeq F^2$ [54]. The mixing between the octet and singlet vector components employed in the construction of the $I = 0$ component of the kaon vector form factors is defined by :

$$\begin{pmatrix} \phi \\ \omega \end{pmatrix} = \begin{pmatrix} \cos\theta_V & -\sin\theta_V \\ \sin\theta_V & \cos\theta_V \end{pmatrix} \begin{pmatrix} v_8 \\ v_0 \end{pmatrix} , \tag{B.5}$$

and we will use ideal mixing, i.e. $\theta_V = 35^\circ$.

References

[1] J. Hisano, T. Moroi, K. Tobe, M. Yamaguchi and T. Yanagida, *Lepton flavor violation in the supersymmetric standard model with seesaw induced neutrino masses*, *Phys. Lett.* **B 357** (1995) 579 [hep-ph/9501407].

[2] J. Hisano, T. Moroi, K. Tobe and M. Yamaguchi, *Lepton-flavor violation via right-handed neutrino Yukawa couplings in supersymmetric standard model*, *Phys. Rev.* **D 53** (1996) 2442 [hep-ph/9510309].

[3] J. Hisano and D. Nomura, *Solar and atmospheric neutrino oscillations and lepton flavor violation in supersymmetric models with the right-handed neutrinos*, *Phys. Rev.* **D 59** (1999) 116005 [hep-ph/9810479].

[4] Y. Kuno and Y. Okada, *Muon decay and physics beyond the standard model*, *Rev. Mod. Phys.* **73** (2001) 151 [hep-ph/9909265].

[5] P. Minkowski, $\mu \to e\gamma$ *at a rate of one out of* 1*-billion muon decays?*, *Phys. Lett.* **B 67** (1977) 421;
M. Gell-Mann, P. Ramond and R. Slansky, *Complex spinors and unified Theories*, in *Supergravity*, P. Van. Nieuwenhuizen and D.Z. Freedman eds., North-Holland, Amsterdam Holland 1979) [Print-80-0576 (CERN)];
T. Yanagida, *Horizontal symmetry and masses of neutrinos*, in *Proceedings of the workshop on the unified theory and the baryon number in the universe*, Tsukuba Japan 13-14 February (1979), O. Sawada and A. Sugamoto eds., KEK;
S.L. Glashow, *Quarks and leptons*, M. Lévy et al. eds., Plenum Press, New York U.S.A. (1980);
R.N. Mohapatra and G. Senjanović, *Neutrino mass and spontaneous parity nonconservation*, *Phys. Rev. Lett.* **44** (1980) 912.

[6] R. Barbieri, D.V. Nanopoulos, G. Morchio and F. Strocchi, *Neutrino Masses in Grand Unified Theories*, *Phys. Lett.* **B 90** (1980) 91;

R.E. Marshak and R.N. Mohapatra, *Selection rules for baryon number nonconservation in gauge models*, invited talk given at *Orbis Scientiae*, Coral Gables, Florida U.S.A., 14–17 January (1980), VPI-HEP-80/02;
T.P. Cheng and L.-F. Li, *Neutrino masses, mixings and oscillations in* SU(2) × U(1) *models of electroweak interactions*, *Phys. Rev.* **D 22** (1980) 2860;
M. Magg and C. Wetterich, *Neutrino mass problem and gauge hierarchy*, *Phys. Lett.* **B 94** (1980) 61;
J. Schechter and J.W.F. Valle, *Neutrino Masses in* SU(2) × U(1) *Theories*, *Phys. Rev.* **D 22** (1980) 2227;
G. Lazarides, Q. Shafi and C. Wetterich, *Proton lifetime and fermion masses in an* SO(10) *model*, *Nucl. Phys.* **B 181** (1981) 287;
R.N. Mohapatra and G. Senjanović, *Neutrino masses and mixings in gauge models with spontaneous parity violation*, *Phys. Rev.* **D 23** (1981) 165;
E. Ma and U. Sarkar, *Neutrino masses and leptogenesis with heavy Higgs triplets*, *Phys. Rev. Lett.* **80** (1998) 5716 [hep-ph/9802445].

[7] Particle Data Group collaboration, W.M. Yao et al., *Review of particle physics*, *J. Phys.* **G 33** (2006) 1.

[8] F. Borzumati and A. Masiero, *Large muon and electron number violations in supergravity theories*, *Phys. Rev. Lett.* **57** (1986) 961.

[9] MEGA collaboration, M.L. Brooks et al., *New limit for the family-number non-conserving decay* $\mu^+ \to e^+\gamma$, *Phys. Rev. Lett.* **83** (1999) 1521 [hep-ex/9905013].

[10] MEG collaboration, S. Ritt, *Status of the MEG expriment* $\mu \to e\gamma$, *Nucl. Phys.* **162** *(Proc. Suppl.)* (2006) 279.

[11] PRIME working group, *Search for the* $\mu - e$ *conversion process at an ultimate sensitivity of the order of* 10^{18} *with PRISM*, unpublished, LOI to J-PARC 50-GeV PS, LOI-25, online at http://psux1.kek.jp/jhf-np/LOIlist/LOIlist.html.

[12] BABAR collaboration, B. Aubert et al., *Search for lepton flavor violation in the decay* $\tau \to \mu\gamma$, *Phys. Rev. Lett.* **95** (2005) 041802 [hep-ex/0502032].

[13] Belle collaboration, K. Abe et al., *A new search for* $\tau \to \mu\gamma$ *and* $\tau \to e\gamma$ *decays at Belle*, hep-ex/0609049.

[14] Belle collaboration, K. Hayasaka et al., *New search for* $\tau \to \mu\gamma$ *and* $\tau \to e\gamma$ *decays at Belle*, arXiv:0705.0650.

[15] S. Banerjee, *Searches for lepton flavor violating decays* $\tau^\pm \to l^\pm\gamma, \tau^\pm \to l^\pm P_0$ *(where* $l^- = e^-, \mu^-$ *and* $P_0 = \pi_0, \eta, \eta'$*) at B-factories: status and combinations*, *Nucl. Phys.* **169** *(Proc. Suppl.)* (2007) 199 [hep-ex/0702017].

[16] Belle collaboration, Y. Miyazaki et al., *Search for lepton flavor violating tau decays into three leptons*, arXiv:0711.2189.

[17] BABAR collaboration, B. Aubert et al., *Improved Limits on the lepton-flavor violating decays* $\tau^- \to l^-\ \ell^+\ell^-$, *Phys. Rev. Lett.* **99** (2007) 251803 [arXiv:0708.3650].

[18] K.S. Babu and C. Kolda, *Higgs-mediated* $\tau \to 3\mu$ *in the supersymmetric seesaw model*, *Phys. Rev. Lett.* **89** (2002) 241802 [hep-ph/0206310].

[19] A. Dedes, J.R. Ellis and M. Raidal, *Higgs mediated* $B^0_{s,d} \to \mu\tau$*,* $e\tau$ *and* $\tau \to 3\mu, e\mu\mu$ *decays in supersymmetric seesaw models*, *Phys. Lett.* **B 549** (2002) 159 [hep-ph/0209207].

JHEP06(2008)079

[20] A. Brignole and A. Rossi, *Lepton flavour violating decays of supersymmetric Higgs bosons*, *Phys. Lett.* **B 566** (2003) 217 [hep-ph/0304081].

[21] E. Arganda and M.J. Herrero, *Testing supersymmetry with lepton flavor violating tau and mu decays*, *Phys. Rev.* **D 73** (2006) 055003 [hep-ph/0510405].

[22] S. Antusch, E. Arganda, M.J. Herrero and A.M. Teixeira, *Impact of θ_{13} on lepton flavour violating processes within SUSY seesaw*, *JHEP* **11** (2006) 090 [hep-ph/0607263].

[23] R. Kitano, M. Koike, S. Komine and Y. Okada, *Higgs-mediated muon electron conversion process in supersymmetric seesaw model*, *Phys. Lett.* **B 575** (2003) 300 [hep-ph/0308021].

[24] E. Arganda, M.J. Herrero and A.M. Teixeira, *$\mu - e$ conversion in nuclei within the CMSSM seesaw: universality versus non-universality*, *JHEP* **10** (2007) 104 [arXiv:0707.2955].

[25] BELLE collaboration, Y. Yusa et al., *Search for neutrinoless decays $\tau \to lhh$ and $\tau \to lV_0$*, *Phys. Lett.* **B 640** (2006) 138 [hep-ex/0603036].

[26] BELLE collaboration, K. Abe et al., *Search for lepton flavor violating τ^- decays into $l^-\eta, l^-\eta'$ and $l^-\pi^0$*, hep-ex/0609013.

[27] BABAR collaboration, B. Aubert et al., *Search for lepton flavor violating decays $\tau^\pm \to l^\pm\pi_0$, $l^\pm\eta, l^\pm\eta'$*, *Phys. Rev. Lett.* **98** (2007) 061803 [hep-ex/0610067].

[28] BELLE collaboration, Y. Miyazaki et al., *Search for lepton flavor violating τ^- decays into $l^-\eta, l^-\eta'$ and $l^-\pi^0$*, *Phys. Lett.* **B 648** (2007) 341 [hep-ex/0703009].

[29] For a review see, for instance, G.L. Kane, C.F. Kolda, L. Roszkowski and J.D. Wells, *Study of constrained minimal supersymmetry*, *Phys. Rev.* **D 49** (1994) 6173 [hep-ph/9312272].

[30] For a review see, for instance, J.R. Ellis, T. Falk, K.A. Olive and Y. Santoso, *Exploration of the MSSM with non-universal Higgs masses*, *Nucl. Phys.* **B 652** (2003) 259 [hep-ph/0210205].

[31] M. Sher, *$\tau \to \mu\eta$ in supersymmetric models*, *Phys. Rev.* **D 66** (2002) 057301 [hep-ph/0207136].

[32] A. Brignole and A. Rossi, *Anatomy and phenomenology of $\mu\tau$ lepton flavour violation in the MSSM*, *Nucl. Phys.* **B 701** (2004) 3 [hep-ph/0404211].

[33] P. Paradisi, *Higgs-mediated $\tau \to \mu$ and $\tau \to e$ transitions in II Higgs doublet model and supersymmetry*, *JHEP* **02** (2006) 050 [hep-ph/0508054].

[34] C.-H. Chen and C.-Q. Geng, *Lepton flavor violation in τ decays*, *Phys. Rev.* **D 74** (2006) 035010 [hep-ph/0605299].

[35] T. Fukuyama, A. Ilakovac and T. Kikuchi, *Lepton flavour violating leptonic/semileptonic decays of charged leptons in the minimal supersymmetric standard model*, hep-ph/0506295.

[36] M. Blanke, A.J. Buras, B. Duling, A. Poschenrieder and C. Tarantino, *Charged lepton flavour violation and $(g-2)_\mu$ in the littlest Higgs model with T-parity: a clear distinction from supersymmetry*, *JHEP* **05** (2007) 013 [hep-ph/0702136].

[37] G. Ecker, J. Gasser, A. Pich and E. de Rafael, *The role of resonances in chiral perturbation theory*, *Nucl. Phys.* **B 321** (1989) 311;
J.F. Donoghue, C. Ramirez and G. Valencia, *The spectrum of QCD and chiral lagrangians of the strong and weak interactions*, *Phys. Rev.* **D 39** (1989) 1947.

JHEP06(2008)079

[38] G.P. Lepage and S.J. Brodsky, *Exclusive processes in perturbative quantum chromodynamics*, *Phys. Rev.* **D 22** (1980) 2157.

[39] Belle collaboration, K. Abe et al., *Search for lepton flavor violating $\tau \to \ell V^0$ decays at Belle*, arXiv:0708.3276.

[40] W. Porod, *SPheno, a program for calculating supersymmetric spectra, SUSY particle decays and SUSY particle production at e^+e^- colliders*, *Comput. Phys. Commun.* **153** (2003) 275 [hep-ph/0301101].

[41] J.A. Casas and A. Ibarra, *Oscillating neutrinos and $\mu \to e, \gamma$*, *Nucl. Phys.* **B 618** (2001) 171 [hep-ph/0103065].

[42] Z. Maki, M. Nakagawa and S. Sakata, *Remarks on the unified model of elementary particles*, *Prog. Theor. Phys.* **28** (1962) 870.

[43] B. Pontecorvo, *Mesonium and antimesonium*, *Sov. Phys. JETP* **6** (1957) 429 [*Zh. Eksp. Teor. Fiz.* **33** (1957) 549]; *Inverse beta processes and nonconservation of lepton charge*, *Sov. Phys. JETP* **7** (1958) 172 [*Zh. Eksp. Teor. Fiz.* **34** (1957) 247].

[44] M.C. González-Garcia and C. Pena-Garay, *Three-neutrino mixing after the first results from K2K and KamLAND*, *Phys. Rev.* **D 68** (2003) 093003 [hep-ph/0306001];
M. Maltoni, T. Schwetz, M.A. Tortola and J.W.F. Valle, *Status of global fits to neutrino oscillations*, *New J. Phys.* **6** (2004) 122 [hep-ph/0405172];
G.L. Fogli, E. Lisi, A. Marrone and A. Palazzo, *Global analysis of three-flavor neutrino masses and mixings*, *Prog. Part. Nucl. Phys.* **57** (2006) 742 [hep-ph/0506083].

[45] G. 't Hooft, *A planar diagram theory for strong interactions*, *Nucl. Phys.* **B 72** (1974) 461;
A two-dimensional model for mesons, *Nucl. Phys.* **B 75** (1974) 461;
E. Witten, *Baryons in the $1/n$ expansion*, *Nucl. Phys.* **B 160** (1979) 57.

[46] S. Peris, M. Perrottet and E. de Rafael, *Matching long and short distances in large-N_c QCD*, *JHEP* **05** (1998) 011 [hep-ph/9805442];
M. Knecht, S. Peris, M. Perrottet and E. de Rafael, *Decay of pseudoscalars into lepton pairs and large-N_c QCD*, *Phys. Rev. Lett.* **83** (1999) 5230 [hep-ph/9908283];
S. Peris, B. Phily and E. de Rafael, *Tests of large-N_c QCD from hadronic tau decay*, *Phys. Rev. Lett.* **86** (2001) 14 [hep-ph/0007338];
B. Moussallam, *A sum rule approach to the violation of Dashen's theorem*, *Nucl. Phys.* **B 504** (1997) 381 [hep-ph/9701400]; *Chiral sum rules for parameters of the order six Lagrangian in the W-Z sector and application to $\pi 0, \eta, \eta'$ decays*, *Phys. Rev.* **D 51** (1995) 4939 [hep-ph/9407402];
M. Knecht and A. Nyffeler, *Resonance estimates of $O(p^6)$ low-energy constants and QCD short-distance constraints*, *Eur. Phys. J.* **C 21** (2001) 659 [hep-ph/0106034];
P.D. Ruiz-Femenía, A. Pich and J. Portolés, *Odd-intrinsic-parity processes within the resonance effective theory of QCD*, *JHEP* **07** (2003) 003 [hep-ph/0306157];
V. Cirigliano, G. Ecker, M. Eidemüller, A. Pich and J. Portolés, *The $< |VAP| >$ Green function in the resonance region*, *Phys. Lett.* **B 596** (2004) 96 [hep-ph/0404004]; *The $< |SPP| >$ Green function and* SU(3) *breaking in $K(l3)$ decays*, *JHEP* **04** (2005) 006 [hep-ph/0503108];
V. Mateu and J. Portolés, *Form factors in radiative pion decay*, *Eur. Phys. J.* **C 52** (2007) 325 [arXiv:0706.1039].

JHEP06(2008)079

[47] J. Bijnens, E. Gamiz, E. Lipartia and J. Prades, *QCD short-distance constraints and hadronic approximations*, *JHEP* **04** (2003) 055 [hep-ph/0304222];
P. Masjuan and S. Peris, *A rational approach to resonance saturation in large-N_c QCD*, *JHEP* **05** (2007) 040 [arXiv:0704.1247].

[48] S. Weinberg, *Phenomenological lagrangians*, *Physica* **A 96** (1979) 327;
J. Gasser and H. Leutwyler, *Chiral perturbation theory to one loop*, *Ann. Phys. (NY)* **158** (1984) 142.

[49] J. Gasser and H. Leutwyler, *Chiral perturbation theory: expansions in the mass of the strange quark*, *Nucl. Phys.* **B 250** (1985) 465.

[50] P. Herrera-Siklódy, J.I. Latorre, P. Pascual and J. Tarón, *Chiral effective lagrangian in the large-N_c limit: the nonet case*, *Nucl. Phys.* **B 497** (1997) 345 [hep-ph/9610549].

[51] R. Kaiser and H. Leutwyler, *Pseudoscalar decay constants at large-N_c*, hep-ph/9806336;
F.-G. Cao and A.I. Signal, *Two analytical constraints on the $\eta\eta'$ mixing*, *Phys. Rev.* **D 60** (1999) 114012 [hep-ph/9908481].

[52] E. Arganda, A.M. Curiel, M.J. Herrero and D. Temes, *Lepton flavor violating Higgs boson decays from massive seesaw neutrinos*, *Phys. Rev.* **D 71** (2005) 035011 [hep-ph/0407302].

[53] P. Paradisi, *Constraints on SUSY lepton flavour violation by rare processes*, *JHEP* **10** (2005) 006 [hep-ph/0505046].

[54] G. Ecker, J. Gasser, H. Leutwyler, A. Pich and E. de Rafael, *Chiral lagrangians for massive spin 1 fields*, *Phys. Lett.* **B 223** (1989) 425;
F. Guerrero and A. Pich, *Effective field theory description of the pion form factor*, *Phys. Lett.* **B 412** (1997) 382 [hep-ph/9707347].

[55] D. Gómez Dumm, A. Pich and J. Portoles, *The hadronic off-shell width of meson resonances*, *Phys. Rev.* **D 62** (2000) 054014 [hep-ph/0003320].

[56] A. Pich and J. Portolés, *Vector form factor of the pion: a model-independent approach*, *Nucl. Phys.* **121** *(Proc. Suppl.)* (2003) 179 [hep-ph/0209224].

JHEP06(2008)079